Published online 6 August 2015 *Nucleic Acids Research, 2015, Vol. 43, No. 20* ***9711–9728***
doi: 10.1093/nar/gkv794

FUS/TLS contributes to replication-dependent histone gene expression by interaction with U7 snRNPs and histone-specific transcription factors

Katarzyna Dorota Raczynska[1,2,*], Marc-David Ruepp[1,3,*], Aleksandra Brzek[2], Stefan Reber[3,4], Valentina Romeo[1,4], Barbara Rindlisbacher[1], Manfred Heller[5], Zofia Szweykowska-Kulinska[2], Artur Jarmolowski[2] and Daniel Schümperli[1,*]

[1]Institute of Cell Biology, University of Bern, Bern, Switzerland, [2]Department of Gene Expression, Institute of Molecular Biology and Biotechnology, Adam Mickiewicz University, Poznan, Poland, [3]Department of Chemistry and Biochemistry, University of Bern, Bern, Switzerland, [4]Graduate School for Cellular and Biomedical Sciences, University of Bern, Bern, Switzerland and [5]Department of Clinical Research, University of Bern, Bern, Switzerland

Received March 17, 2015; Revised July 18, 2015; Accepted July 26, 2015

ABSTRACT

Replication-dependent histone genes are up-regulated during the G1/S phase transition to meet the requirement for histones to package the newly synthesized DNA. In mammalian cells, this increment is achieved by enhanced transcription and 3′ end processing. The non-polyadenylated histone mRNA 3′ ends are generated by a unique mechanism involving the U7 small ribonucleoprotein (U7 snRNP). By using affinity purification methods to enrich U7 snRNA, we identified FUS/TLS as a novel U7 snRNP interacting protein. Both U7 snRNA and histone transcripts can be precipitated by FUS antibodies predominantly in the S phase of the cell cycle. Moreover, FUS depletion leads to decreased levels of correctly processed histone mRNAs and increased levels of extended transcripts. Interestingly, FUS antibodies also co-immunoprecipitate histone transcriptional activator NPAT and transcriptional repressor hnRNP UL1 in different phases of the cell cycle. We further show that FUS binds to histone genes in S phase, promotes the recruitment of RNA polymerase II and is important for the activity of histone gene promoters. Thus, FUS may serve as a linking factor that positively regulates histone gene transcription and 3′ end processing by interacting with the U7 snRNP and other factors involved in replication-dependent histone gene expression.

INTRODUCTION

The expression of the metazoan replication-dependent histone genes is cell cycle-regulated to meet the requirement for histones to package the newly synthesized DNA during the S phase of the cell cycle. Histone mRNA levels increase ∼35-fold during the G1/S phase transition and rapidly drop again at the end of S phase (1,2). The general transcription factor NPAT is known to bind to replication-dependent histone gene promoters and to activate transcription during S phase (3), resulting in a ∼5-fold increase in histone gene transcription (2). Moreover, the S phase-dependent increment of replication-dependent histone mRNAs is also due to more efficient histone RNA 3′ end processing. In contrast, the drop in histone mRNA levels at the S/G2 transition is mostly due to a rapid destabilization of the existing mRNAs (2).

Replication-dependent histone transcripts are not processed at the 3′ end by cleavage coupled to polyadenylation like the majority of eukaryotic pre-mRNAs. Instead, histone mRNA 3′ end processing consists of a single cleavage that is carried out by the endonuclease CPSF73 and mediated by a subset of specialized factors that recognize specific elements on the nascent transcripts (4–6). Histone pre-mRNAs end in a conserved stem loop recognized and bound by the hairpin- or stem loop-binding protein (HBP/SLBP) that defines the cleavage site a few nucleotides downstream, usually after a CA dinucleotide (4,7–8). The other determinant of the cleavage site is the U7 small ribonucleoprotein (U7 snRNP) that binds by basepairing of the 5′ end of U7 snRNA to the histone downstream element (HDE) located 3′ of the cleavage site (9,10).

*To whom correspondence should be addressed. Tel: +41 31 631 4675; Fax: +41 31 631 4431; Email: daniel.schuemperli@izb.unibe.ch
Correspondence may also be addressed to Katarzyna Dorota Raczynska. Tel: +48 61 829 5953; Fax: +48 61 829 5949; Email: doracz@amu.edu.pl
Correspondence may also be addressed to Marc-David Ruepp. Tel: +41 31 631 4348; Fax: +41 31 631 4887; Email: marc.ruepp@dcb.unibe.ch
Present address: Barbara Rindlisbacher, Institute of Clinical Chemistry, Inselspital, University of Bern, Bern, Switzerland.

The U7 snRNP consists of an approximately 60-nucleotide U7 snRNA (11–13) and an unusual ring of Sm/Lsm proteins in which the two spliceosomal proteins SmD1 and SmD2 are replaced by the Sm-like proteins Lsm10 and Lsm11 (14,15). Lsm11 contains an extended N terminus that is necessary for processing and forms a platform for interactions with other factors. In particular, the U7-specific Lsm11 protein binds to a 100 kDa zinc-finger protein (ZFP100) which in turn interacts with SLBP and stabilizes the complex (16–18). Lsm11 also binds to another histone-specific processing factor, FLASH (19–21) and to the 68 kDa subunit of mammalian cleavage factor I (22). Together, the U7 snRNP-specific protein Lsm11 and FLASH form a binding platform to recruit a heat-labile processing factor (HLF) that contains symplekin, CstF64 and other components of cleavage/polyadenylation machinery, including the endonuclease CPSF73 (1,21,23–25).

Two of the histone processing factors are known to be cell cycle-regulated. These are SLBP (26) and the HLF through its CstF64 subunit (1,25). Moreover, the U7 snRNP has been shown to play an additional regulatory role. Together with the hnRNP protein UL1, it acts to repress histone gene transcription outside of S phase (27).

By using different affinity purification strategies for U7 snRNA, we have now identified fused in sarcoma/translocated in liposarcoma (FUS/TLS; named FUS thereafter) as a new factor involved in replication-dependent histone gene expression. FUS belongs to the FET family which includes three highly conserved, abundant and ubiquitously expressed RNA-binding proteins: FUS, EWS and TAF15 (28). FUS is predominantly present in the nuclear matrix, although it is also found in cytoplasmic fractions and is supposed to participate in nucleo-cytoplasmic shuttling (29). FUS binds to both ssDNA and dsDNA and is able to promote DNA annealing and D-loop formation which implies a role in genomic maintenance, DNA recombination and the DNA repair pathway (30–32). FUS is also capable of binding RNA both in the nucleus and cytoplasm, and thus a function for FUS in RNA transport has been suggested (29,33–36). Similar to other FET proteins, FUS associates with the transcription factor IID complex (TFIID), as well as directly with RNA polymerase II (RNAP2) (37) and can regulate transcription of RNAP2 genes (30,38–40). Interestingly, FUS was also shown to act as a repressor of transcription for all three classes of RNA polymerase III promoters (41). Moreover, FUS plays a role in splicing and alternative splicing; its presence was confirmed in the spliceosome and an association with several spliceosomal small nuclear ribonucleoproteins and SR proteins has been detected (34–35,42–49). Additionally, FUS may play a role in miRNA processing as it has been found in the large Drosha microprocessor complex (50). Several FUS/TLS mutations have been found in familial forms of amyotrophic lateral sclerosis (ALS) and frontotemporal lobar degeneration (FTLD), implicating a pathogenic role of this protein in neurodegenerative diseases (28,51–55).

In this paper, we show that FUS is associated with the U7 snRNP/U7 snRNA and replication-dependent histone gene transcripts (H2A, H2B, H3 and H4), predominantly during the S phase of the cell cycle. Moreover FUS depletion by RNAi induces a decrease of correctly processed histone mRNAs and an increased level of extended transcripts. The opposite effect can be observed in FUS overexpressing cells. Interestingly, the histone transcriptional activator NPAT and the transcriptional repressor hnRNP UL1 are also co-precipitated by anti-FUS antibodies in a cell cycle-dependent manner. Furthermore, we show, by chromatin immunoprecipitation experiments (ChIP), that FUS binds to replication-dependent histone gene promoters and enhances the binding of RNAP2 to these promoters during S phase. FUS depletion also affects the activities of histone gene promoters in a reporter gene assay. This strongly indicates that FUS is involved in the regulation of histone gene transcription and 3′ end processing.

MATERIALS AND METHODS

Cell culture, synchronization and cell cycle analysis

HeLa or HEK 293T cells were grown in Dulbecco's modified Eagle medium with L-glutamine and 4.5 g/L glucose (DMEM; Lonza) supplemented with 10% fetal calf serum (Gibco) and antibiotics (100 U/ml penicillin, 100 μg/ml streptomycin, 0.25 μg/ml amphotericin B (Sigma)) at 37°C in a moist atmosphere containing 5% CO_2.

Synchronization of HEK 293T and HeLa cells in G2/M was done by addition of 200 ng/ml nocodazole (Sigma-Aldrich) to the medium for 18 h. For G2, G1 and S phase synchronization, HEK 293T cells were arrested in G2/M by addition of 200 ng/ml nocodazole and then collected 2, 5 and 15 h after release, respectively. For S phase synchronization HeLa cells were blocked first by 2 mM thymidine (Sigma-Aldrich) for 17 h, then released for 12 h, blocked again by 400 μM mimosine (Sigma-Aldrich) for 14 h and collected 5 h after release. For G1 synchronization, HeLa cells were blocked first by 2 mM thymidine for 24 h, then released for 3 h, blocked again by 0.1 μM nocodazole for 12 h and collected 5 h after release.

For cytofluorometric analysis, the cells were trypsinized, washed with phosphate-buffered saline (PBS) and fixed by dropwise addition of ice-cold 70% ethanol. Before staining with propidium iodide (PI), the cells were washed twice with PBS and resuspended in PI-staining solution (0.1% Triton X-100 in PBS, 0.2 mg/ml RNase A (Termo Scientific), 0.02 mg/ml propidium iodide (Sigma)) and incubated for at least 30 min at room temperature in the dark. Cell cycle profiles were analyzed by cytofluorometry with a BD FACS Aria III flow cytometer and the data was processed with FACSDiva Version 6.1.3 software. The quality of cell synchronizations was additionally assessed by measuring the levels of cyclin B1 and β-actin on Western blots.

For cell proliferation tests, the cells were plated in triplicate in 12-well plates at 50 000 cells/well. Then cell counts and viability were measured every 24 h for 6 days by using a Countess™ Automated Cell Counter (Life Technologies). The results are shown as cell proliferation curves.

Plasmid construction, lentiviral vetor production and cell transduction

Lentiviral expression vectors encoding FLAG-tagged FUS and enhanced blue fluorescence protein (EBFP) were con-

structed as follows: annealed and kinased oligos encoding a GSG15-FLAG tag followed by the stop codon TAA were cloned into the BamHI and NotI sites of pCDH-CuO-MCS-EF1-RFP (System Biosciences, Montain View, CA, USA) to create pCDH-CuO-MCS-GSG15-FLAG-EF1-RFP. PCR (polymerase chain reaction) amplified FUS and EBFP cDNAs were then cloned into the XbaI and BamHI sites of this vector. The FUS PCR product was amplified from the full length ImaGenes Clone IRAUp969F059D. PCR amplified Flag-mLsm11 cDNA was introduced into pLVttR-KRAB-dsRed (56) vector by using MluI/SmaI sites to create pLV-ttR-Flag-Lsm11-dsRed.

Expression vectors for normal and MS2-tagged U7 snRNAs were constructed by cloning the wild type mouse U7 snRNA sequence into pSP64 by using HpaI and StuI restriction sites and subsequent addition of an MS2 loop at the 5′ end of U7 snRNA by amplification with specific primers. Next the U7 snRNA expression cassette was amplified with primers adding flanking SfuI and ClaI restriction sites, and ligated into a ClaI-cut pWPTS-eGFP vector (57).

The vector for the inducible FUS knockdown was created by digesting the pSUPuro FUS plasmid with BstXI and SalI to isolate the fragment containing the H1 promoter followed by the shRNA cassette. This fragment was then cloned into pLV-TH by using the same restriction sites as described in (58). pSUPuro-FUS was cloned by inserting double-stranded oligos into pSUPERpuro between the BglII and HindIII sites as described (59,60). The shRNA expressed from pSUPuro FUS is targeting nucleotides 535–553 of FUS mRNA, numbering according to NM_004960, (GGACAGCAGCAAAGCTATA). All primer sequences used for cloning are available on request.

Virus production for protein expression was essentially performed as follows: HEK 293T cells were transfected with pCDH-CuO-FUS-GSG15-FLAG-EF1-RFP or pCDH-CuO-EBFP-GSG15-FLAG-EF1-RFP, pLV-ttR-Flag-Lsm11-dsRed or pWPTS-EF1α-(MS2)U7snRNA-eGFP supplemented with pLpCMVDR8.91 and pMD2.G according to established methods (56). Lentiviral supernatants were collected 48, 72 and 96 h post transfection and filtered through a 0.45 μM polyethersulfone sterile filter (Millipore). For transduction, HEK 293T or HeLa cells were incubated with lentiviral supernatants supplemented with 5 μg/ml polybrene (hexadimethrine bromide, Sigma Aldrich). After 7 h, polybrene was diluted to 2.5 μg/ml by the addition of fresh DMEM/10% FBS and the procedure was repeated for two days. After expansion of the transduced cells, highly RFP positive cells were collected by fluorescence-activated cell sorting (FACS) to yield a transduced cell pool. The inducible FUS and control knockdown cell lines were generated according to the published protocol (56) as described in (58).

To construct histone promoter reporter plasmids, the promoter regions including the 5′UTRs were amplified from HeLa genomic DNA by PCR. The forward and the reverse primers (listed in Supplementary Table S3) contained BglII and XhoI restriction enzyme sites, respectively, and the PCR-amplified fragments were cloned into the BglII and XhoI sites of pcDNA-HA-EGFP enhanced green fluorescence protein (EGFP) (14) to replace the human Cytomegalovirus (CMV) promoter with the corresponding histone promoter amplicons. The Hist3H2A construct encompasses nucleotides -649 to +42, the Hist2H3C construct nucleotides from -600 to +36, the Hist2H4 construct nucleotides -628 to +28, and the Hist1H3C and Hist3H3 constructs 645 and 660 nucleotides upstream of the start codon, respectively.

Antibodies

The following primary antibodies were used in this work: anti-Lsm11, anti-hnRNP UL1, anti-RPB2 (Abcam), anti-ZN473 (Abgent), anti-symplekin, anti-V5, anti-FUS Ab1, anti-FUS Ab2, anti-TAF15 (Bethyl Laboratories), anti-SLBP, anti-Lsm10, anti-lamin A/C, anti-HA, anti-Cyclin B1, anti-GADPH, antiH2A, anti-H2B, anti-H2A.Z, anti-H4 (Santa Cruz Biotechnology), anti-β-actin (MP Biomedicals), anti-Maltose Binding Protein, anti-FLAG (Sigma Aldrich), Y12 monoclonal antibody (recognizing SmB/B', SmD1) as described in (61). The following secondary antibodies were used: goat anti-rabbit IgG-HRP, donkey anti-goat IgG-HRP, goat anti-mouse IgG-HRP (Santa Cruz Biotechnology).

A polyclonal rabbit anti-FUS antibody was prepared as follows: a cDNA fragment, amplified by PCR, encoding the first 286 amino acids of FUS was cloned between the EcoRI and XhoI sites of pET28a. The recombinant protein was expressed in BL21(DE3) Codon Plus RIPL and purified under denaturing conditions over Ni-NTA beads according to the manufacturer's instructions. The purified protein was dialyzed against PBS, and rabbits were immunized with the purified protein in combination with GERBU Adjuvant LQ. Primer sequences used for cloning and are available on request.

RNA isolation, cDNA preparation, PCR and qPCR, primer extension

RNA was isolated from cells with TRIZOL reagent (0.8 M guanidine thiocyanate, 0.4 M ammonium thiocyanate, 0.1 M sodium acetate pH 5.0, 5% V/V glycerol, 38% V/V saturated acidic phenol, 5 mM EDTA, 0.5% sodium lauroylsarcosine, in diethylpyrocarbonate-treated water (DEPC)). The samples were vortexed vigorously and kept for 10 min at room temperature. Then 0.5 volume of chloroform was added, throughly mixed and after an additional incubation of 5 min, centrifuged for 5 min at 13'600 g. The aqueous phase was transferred to a fresh tube and re-extracted with 1 volume of chloroform. The aqueous phase was collected, and the RNA was precipitated by addition of 1 volume of isopropanol and overnight storage at -20°C. The precipitated RNA was centrifuged for 45 min at 16'100 g. The pellet was washed with 70% ethanol, centrifuged for 10 min at 16'100 g, air-dried and resuspended in RNAse-free water. Usually 30 μg of RNA was treated with 2U TURBO DNase (Ambion) in TURBO DNase buffer in the presence of 20U RNasin (Promega) for 1 h at 37°C followed by standard phenol-chloroform extraction and ethanol precipitation.

First strand cDNAs were synthesized in 50 μl reactions with 3 μg of RNA by using 400 ng random hexamers as

primers and 200U Superscript III Reverse Transcriptase (SSIII RT, Invitrogen), according to the manufacturer's protocol. If not mentioned, 1 μl of cDNA template was then used for each PCR/qPCR amplification with gene-specific oligonucleotide primer pairs. PCR amplifications were carried out in 25 μl reactions containing 2.5 μl of PCR buffer with $MgCl_2$, nucleotide mix (0.2 mM each dNTP (Roche)), 0.5 μM primers and DreamTaq DNA Polymerase (5U/μl, (Thermo scientific)). The samples were incubated for the indicated number of cycles under the following conditions: 94°C for 2 min, each cycle: 94°C for 30 s, 50°C for 30 s, 72°C for 1 min and completed by incubation for 10 min at 72°C. For qPCR amplifications, 10 μl reaction mix contained 5 μl of Power SYBR Green PCR Master Mix (Applied Biosystems), 4 μl of 0.5 mM primers mix and 1 μl of 4x diluted cDNA template. The qPCR was performed for 40 cycles under the following cycling conditions: 95°C for 10 min, 40 cycles of 95°C for 15 s, 60°C for 1 min (Applied Biosystems 7900 HT thermocycler). Primers used for PCR and qPCR are listed in the Supplementary Tables S2 and S3. The statistical significance of qPCR results was determined by Student's T test.

For snRNA analysis, cDNA was synthesized in a coupled polyadenylation reverse transcription reaction by using 2 μg of RNA for 1 h at 37°C in RT buffer (10 mM Tris-HCl pH 8.0, 75 mM KCl, 10 mM DTT, 70 mM $MgCl_2$, 20U RNasin, 2.5 mM of all four deoxynucleoside triphosphates, 0.5 mM of rATP, 800 ng of anchored oligo(dT) primer) supplemented with 200U Superscript III reverse transcriptase (Invitrogen) or AffinityScript reverse transcriptase (Agilent) and 5U *E. coli* Poly(A) polymerase (PAP, New England Biolabs). Reactions were heat-inactivated for 10 min at 85°C. Then, 4 μl of the 9x diluted cDNA template per reaction were used for each qPCR amplification with a reverse primer complementary to the anchored sequence and a probe-specific forward primer (600 nM each) (Suplementary Table S3).

For primer extension experiments, the U7wt-PEX primer (Suplementary Table S3) complementary to an internal sequence of U7 snRNA was labeled at the 5′ end with [γ-^{32}P]ATP (Hartmann Analytic) by polynucleotide kinase (PNK) in PNK buffer (New England Biolabs) for 1 h at 37°C. Next, 10 pmoles of labeled primer were hybridized with 3 μg of RNA in a thermocycler by heating to 95°C and slow cooling to 45°C. The primer extension reaction was then carried out for 2 h at 37°C with 200U Superscript III reverse transcriptase (Invitrogen) in RT buffer in the presence of 10 mM DTT, 0.5 mM of all four deoxynucleoside triphosphates and 20U RNasin. Primer extension products were separated on 12% polyacrylamide/7M urea gels in Tris-borate/EDTA buffer, pH 8.3 in the presence of radiolabeled size marker (HpaII digested pBR 322 plasmid) and detected with the image analyzer (FLA-5000, FujiFilm).

Nuclear and cytoplasmic protein extract preparation

Cells were harvested by trypsinization, washed with PBS, resuspended in Lysis Buffer (10 mM HEPES pH 7.9, 60 mM KCl, 1 mM EDTA, 1 mM $MgCl_2$, 1 mM DTT, 0.2% NP40, 1x EDTA-free protease inhibitor (Roche)) and incubated on ice for 2 min. After centrifugation for 1 min at 800 g, the supernatant containing cytoplasmic proteins was collected in a new tube; the pellet was washed with washing buffer (10 mM HEPES pH 7.9, 60 mM KCl, 1 mM $MgCl_2$, 1 mM DTT, 1x EDTA-free protease inhibitor), centrifuged as previously and then resuspended in nuclear buffer (250 mM Tris-HCl pH 7.9, 60 mM KCl, 1 mM EDTA, 1 mM $MgCl_2$, 1 mM DTT, 0.2% NP40, 1x EDTA-free protease inhibitor (Roche), 10% glycerol) and shaken vigorously for 30 min at 4°C. After centrifugation for 30 min at 16 000 g, the supernatant containing nuclear proteins was collected in a new tube. The quality of the nucleo-cytoplasmic separation was assessed by Western blot analysis by detection of β-actin and lamin A/C.

Immunoprecipitation, RNA immunoprecipitation

For co-immunoprecipitation, the protein extracts from cells overexpressing FLAG-tagged proteins (prepared as described above) were gently rotated overnight at 4°C with anti-FLAG antibody-coupled magnetic beads (Sigma), then washed four times with Lysis Buffer and eluted with 3xFLAG peptide or by boiling in Sample Buffer (50 mM Tris–HCl pH 6.8, 10% glycerol, 2% SDS, 10 mM DTT, 0.1% bromophenol blue). As negative control, protein extract from non-transduced cells was used. Alternatively, protein extracts were incubated with Dynabeads Protein G coupled to 40 μg protein-specific antibodies for 1.5 h at 4°C and eluted by boiling in Sample Buffer. As negative control, Dynabeads Protein G coupled to either mouse IgG or rabbit IgG were used. After elution, the immune complexes were separated by SDS-polyacrylamide gel electrophoresis (PAGE), transferred to polyvinylidene difluoride (PVDF) membrane (Millipore) and detected by incubation with corresponding species-specific horseradish peroxidase (HRP)-coupled secondary antibody and by using the enhanced chemiluminescence method (ECL, GE Healthcare).

For RNA immunoprecipitation (RIP) experiments, the nuclear and cytoplasmic protein extracts were subjected to immunoprecipitation essentially as described above. For the RIP shown in Figure 2, nuclear extracts from IPRACELL (Mons, Belgium) were used. After washing the immunoprecipitated complexes with TBS-0.05% NP-40, the co-precipitated RNAs were eluted from the beads with TRIZOL and used for cDNA synthesis followed by qPCR as described above. As input, the same amounts of extracts were directly added to TRIZOL. Primers used are listed in Supplementary Table S2.

Protein overexpression in bacteria

The *Escherichia coli* strains BL21-CodonPlus(De3)-RIPL and BL21-CodonPlus(De3)-RIL were transformed with pMal-derived plasmids encoding MS2-MBP fusion protein (62) or MBP fused in frame to full length FUS protein or to a ΔNT FUS derivative lacking the first 165 amino acid codons, respectively. Primer pairs used for cloning FUS proteins in the pMal vector were designed to contain NcoI and EcoRV restriction sites (sequences available on request). Bacterial cultures were grown at 37°C with continuous shaking in Luria-Bertani medium (LB) containing

50 μg/ml ampicillin and 34 μg/ml chloramphenicol to an OD_{600} of 0.6 to 0.8, and protein overexpression was induced for 2.5 h by adding 0.3 mM IPTG (MS2-MBP) or for 5 h by adding 0.1 mM IPTG (MBP-FUS) to the culture. After this time, the cells were harvested by centrifugation for 30 min at 3000 g, resuspended in Sonication Buffer (20 mM Tris-HCl pH 7.5, 200 mM NaCl; 1x EDTA-free protease inhibitor (Roche)) and sonicated with a Bioruptor® Plus Sonicator (Diagenode) for 15 cycles at high intensity: 30 s ON/30 s OFF at 4°C. The cell debris were removed by centrifugation for 15 min at 16 000 g, and supernatants were incubated with amylose resin (New England Biolabs) with gentle rotation for 4 h at 4°C. After this time, the resins were washed three times with Column Buffer (CB, 20 mM Hepes-KOH pH 7.9, 150 mM NaCl, 0.5% NP-40, 1x EDTA-free protease inhibitor (Roche)) and eluted with 10 mM maltose. After purification, the proteins were analyzed by SDS-PAGE. For MS2-MBP purification, the amylose resin was additionally washed with Wash Buffer (WB, 5 mM Na_2HPO_4/NaH_2PO_4, (pH 7.0)) and then the fusion protein was eluted by 15 mM maltose in WB buffer and loaded twice onto a heparin resin (GE Healthcare). The heparin column was washed twice by WB buffer followed by elution using Elution Buffer (EB, 20 mM Hepes-KOH pH 7.9, 100 mM KCl, 15% glycerol, 0.5 mM DTT, 0.2 M PMSF, 1x EDTA-free protease inhibitor (Roche)). The eluted MS2-MBP protein was quantitated and analyzed by SDS-PAGE.

Affinity purification

Purified MS2-MBP fusion protein was bound to amylose resin by overnight incubation at 4°C in MBP Column Buffer (20 mM Tris-HCl pH 7.4, 150 mM NaCl, 1 mM EDTA, 1x EDTA-free protease inhibitor (Roche)) with gentle rotation followed by washing three times with MBP Wash Buffer (20 mM Tris-HCl pH 7.4, 60 mM NaCl, 1 mM EDTA, 1x EDTA-free protease inhibitor (Roche)). Cytoplasmic and nuclear protein extracts (prepared as described above) from cells expressing MS2-tagged U7 snRNA or additional copies of the normal U7 snRNA were loaded onto the MS2-MBP-bound resin and incubated for 4 h at 4°C with gentle rotation. Purified complexes were eluted from the resin by 10 mM maltose in MBP Column Buffer for 30 min at 4°C, concentrated, and aliquots were analyzed by Western blot. Samples were either directly submitted to mass spectrometric analysis or separated on a SDS polyacrylamide gel followed by silver staining. In the latter case, selected bands were cut from the gel and submitted to mass spectrometric analysis. In some cases, probes were first loaded onto 10–50% continuous glycerol gradients (Biocomp Gradient Station) and centrifuged for 36 h at 36 000 g. The gradients were collected into 17 fractions (of 0.68 ml) and selected fractions were used for affinity purification.

As a second approach to enrich proteins associated with U7 snRNA, HeLa nuclear extracts were incubated with a biotinylated 2′-O-methyl RNA oligonucleotide complementary to U7 snRNA (AS-U7) or to 7SL RNA (AS-7SL) for 30 min at 30°C followed by binding to streptavidin-coated Dynabeads for 1.5 h at 4°C. After five subsequent washes, the beads were boiled in sample buffer, and the precipitated material was separated by SDS-PAGE and analyzed by Western blot.

Proteomic analysis by mass spectrometry

Gel slices were destained as described (63), and proteins were digested with sequencing grade trypsin with the addition of 0.01% ProteaseMax (Promega) as described (64). For in-solution digestion, samples were prepared as described (65). Peptides were separated by reversed nano-liquid chromatography using a 20 or 60 min gradient according to the expected sample complexity. Peptide sequencing was performed on a LTQ-orbitrap XL system and data interpretation done as described (64).

Chromatin immunoprecipitation

HEK 293T cells and HEK 293T cells overexpressing FLAG-FUS and FLAG-EBFP and FUS-depleted cells were synchronized to G1 and S phase (as described above). Cells were trypsinized, washed with PBS and cross-linked with 1% formaldehyde for 10 min followed by quenching with 125 mM glycine for 5 min. The fixed cells were washed twice with PBS and lysed in Cell Lysis Buffer (10 mM Tris-HCl pH 8.1, 10 mM NaCl, 1.5 mM $MgCl_2$, 0.5% NP-40, 1x EDTA-free protease inhibitor (Roche)) for 15 min on ice and then centrifuged at 800 g for 5 min at 4°C. The pellet was resuspended in Nuclear Lysis Buffer (50 mM Tris-HCl pH 8.1, 5 mM EDTA, 0.5% sarkosyl, 1x EDTA-free protease inhibitor (Roche)) and moved to DNA LoBind Tubes (Eppendorf). The nuclear lysate was sonicated with a Bioruptor® Plus Sonicator (Diagenode) to generate DNA fragments between 200 bp and 700 bp (usually 17 cycles, at high intensity: 30 s ON/30 s OFF at 4°C). Each time, the sizes of DNA fragments were verified by agarose gel electrophoresis. After sonication, the cell debris were removed by centrifugation at 4000 g for 5 min at 4°C, the concentration of DNA was measured, and the supernatants were diluted 10 times with Dilution Buffer (16.7 mM Tris-HCl pH 8.1, 167 mM NaCl, 12 mM EDTA, 1.1% Triton X-100, 0.01% SDS, 1x EDTA-free protease inhibitor (Roche)). An amount of 25 μg of chromatin was immunoprecipitated overnight at 4°C with: a) 10 μl of ANTI-FLAG® M2 Magnetic Beads; b) 5 μg of anti-RPB2 antibody (Abcam, ab10338) previously conjugated for 1 h at 4°C with gentle rotation with 15 μl of Dynabeads® Protein G (Life Technologies); c) 15 μl of non-conjugated beads. One tenth of the chromatin used for immunoprecipitation was kept in a separate tube as input. After immunoprecipitation, beads were washed three times with Low Salt Wash Buffer (20 mM Tris-HCl pH 8.1, 150 mM NaCl, 2 mM EDTA, 0.1% SDS, 1% Triton X-100), three times with High Salt Wash Buffer (20 mM Tris-HCl pH 8.1, 500 mM NaCl, 2 mM EDTA, 0.1% SDS, 1% Triton X-100), three times with LiCl Wash Buffer (10 mM Tris-HCl pH 8.1, 250 mM LiCl, 1 mM EDTA, 1% NP-40, 1% sodium deoxycholate) and three times with TE Buffer (10 mM Tris-HCl pH 8.0, 1 mM EDTA), each time for 5 min on a rotating wheel at 4°C. After washing, the captured chromatin was eluted by addition of Elution Buffer (1% SDS, 100 mM $NaHCO_3$, pH 8.2) followed by vigorous shaking for 15 min at 30°C. At

this stage, inputs were included and treated identically as immunoprecipitated probes. The eluted probes were transferred to new tubes and reverse-cross-linked overnight at 65°C with NaCl at 0.3 M final concentration. Then the probes were digested for 2 h at 50°C by 40 μg/ml Proteinase K (Thermo Scientific) and 20 μg/ml RNase A (Thermo Scientific) in PK Buffer (50 mM Tris-HCl pH 7.5, 25 mM EDTA, 1.25% SDS). The DNA samples were extracted with a Syngen PCR ME Mini Kit following the manufacturer's instruction. The precipitated DNAs were used for qPCR analysis; primer pairs encompassing the promoter regions, open reading frames and 3′ UTR regions of histone genes are listed in Supplementary Table S4. The quantitative analysis of precipitated material was shown as a fold change normalized to input and relative to FLAG-EBFP or shFUS cells not treated with doxycycline. Identically treated samples from non-conjugated beads and HEK 293T cells were used to determine non-specific background. The statistical significance of qPCR results was determined by Student's T test.

Histone promoter reporter assays

HeLa cells with doxycycline-inducible FUS or control depletion were induced by incubation in DMEM supplemented with 10 μg/ml doxycycline (Sigma). For HeLa cells without inducible depletion system, 5×10^5 cells were seeded into a T25 flask and transfected on the next day with 1 μg of pSUPuro scr (control depletion) (66) or pSUPuro FUS plasmid. One day after transfection, transfected cells were selected by adding 1.5 μg/ml puromycin (Santa Cruz) for 24 h.

For the promoter reporter assays, 5×10^5 cells on day two of depletion were seeded into a T25 flask and co-transfected on the next day with 1 μg reporter plasmid and 0.5 μg pBS-β-globin (67) to normalize for variations in transfection efficiency. Two days post transfection (day 4 of FUS depletion) the cells were harvested. Briefly, 1×10^6 cells were removed to verify FUS depletion by Western blotting. Total RNA was isolated from the remaining cells by guanidinium thiocyanate:phenol:chlorophorm extraction (58). After DNase treatment with the TURBO DNA-free™ Kit (Ambion, Life Technologies™), 1 μg total RNA was reverse-transcribed with 450 ng random hexamers, 1 x AffinityScript RT buffer, 1 μl AffinityScript Multiple Temperature Reverse Transcriptase, 0.4 mM dNTPs, and 10 mM DTT (Agilent Technologies) according to the manufacturer's manual. To confirm successful DNase digestion, controls lacking reverse transcriptase were made. The cDNA was diluted to a RNA concentration of 8 ng/μl. Quantitative real-time PCR was performed using 3 μl cDNA, 1 x MESA GREEN qPCR Mastermix Plus for SYBR® Assay No ROX (Eurogentec) and 8 μM each of forward and reverse primer in a total volume of 15 μl. Samples were measured in duplicates in a Rotorgene6000 (Corbett) by using the following cycling conditions: 95°C, 5 min; 95°C, 15 s; 60°C 1 min; 40 cycles. A melting curve was recorded from a temperature gradient from 65°C to 95°C, 5 s/°C. The analyses were performed as described in (58). Primers used for qPCR are listed in Supplementary Table S3 (β-globin, EGFP). The statistical significance of qPCR results was determined by Student's T test.

RESULTS

FUS interacts with the U7 snRNP *in vivo*

The first indication that FUS could be involved in histone gene expression came from a search for novel proteins interacting with the U7 snRNP. For this purpose, we developed several enrichment schemes. In a first approach, we tagged the 5′ end of U7 snRNA with one, two or three copies of the MS2 RNA hairpin. These constructs were stably introduced into HeLa cells by lentiviral transduction. All three U7 snRNAs were expressed, but with decreasing efficiency as more MS2 sites were inserted (Supplementary Figure S1). This decrease may have been due to reduced assembly into snRNPs. Nuclear extracts from the resulting cell lines were subjected to affinity purification by using a recombinant maltose-binding protein (MBP):MS2 coat protein fusion and amylose resin. As an independent approach, we used a biotinylated oligonucleotide complementary to the 5′ end of U7 snRNA and streptavidin beads to purify endogenous U7 snRNPs. Additionally or in combination with one of the above methods, we collected U7 snRNP-enriched fractions from glycerol gradients. With these different approaches, we performed several U7 purifications that were subjected to proteomic analysis by mass spectrometry either directly or from gel slices after electrophoresis. Interestingly, the FUS protein could be identified in a total of 16 different U7-enriched fractions obtained by these various methods (Supplementary Table S1). FUS was also identified twice in negative controls, probably because of an unspecific interaction with the affinity column (MS2-MBP bound to amylose beads).

The presence of FUS and selected proteins involved in replication-dependent histone gene expression was confirmed by Western blot in several of the the U7 snRNP-enriched fractions. As an example, histone-specific proteins (Lsm10, SLBP, ZFP100) as well as symplekin (a component of the HLF) were significantly enriched in a fraction obtained by affinity purification based on 1x MS2-tagged U7 snRNA (Figure 1A). Importantly, probing the blot with anti-FUS antibody confirmed the presence of FUS in the purified fraction. However FUS was also retained, albeit more weakly, from an extract of non-transduced HeLa cells; this indicated that FUS can also interact non-specifically with either the affinity column or MS2-MBP.

Similarly, FUS could be highly enriched by affinity purification of U7 snRNPs with a biotinylated 2′-O-methyl RNA antisense oligonucleotide (AON) complementary to the 5′ end of U7 snRNA (AS-U7) (Figure 1B). As expected, AS-U7 also precipitated SmB/B', a member of the Sm ring of the U7 snRNP. As negative control, an AON directed against 7SL RNA precipitated only faint traces of FUS and SmB/B'.

The FUS:U7 snRNP interaction was further confirmed by immunoprecipitation of cytoplasmic (Cyt) and nuclear (Nuc) extracts from HeLa cells stably overexpressing FLAG-Lsm11 with anti-FLAG-coupled magnetic beads and re-elution by a 3xFLAG peptide (Figure 1C). This experiment also indicated that FUS itself (see input) but

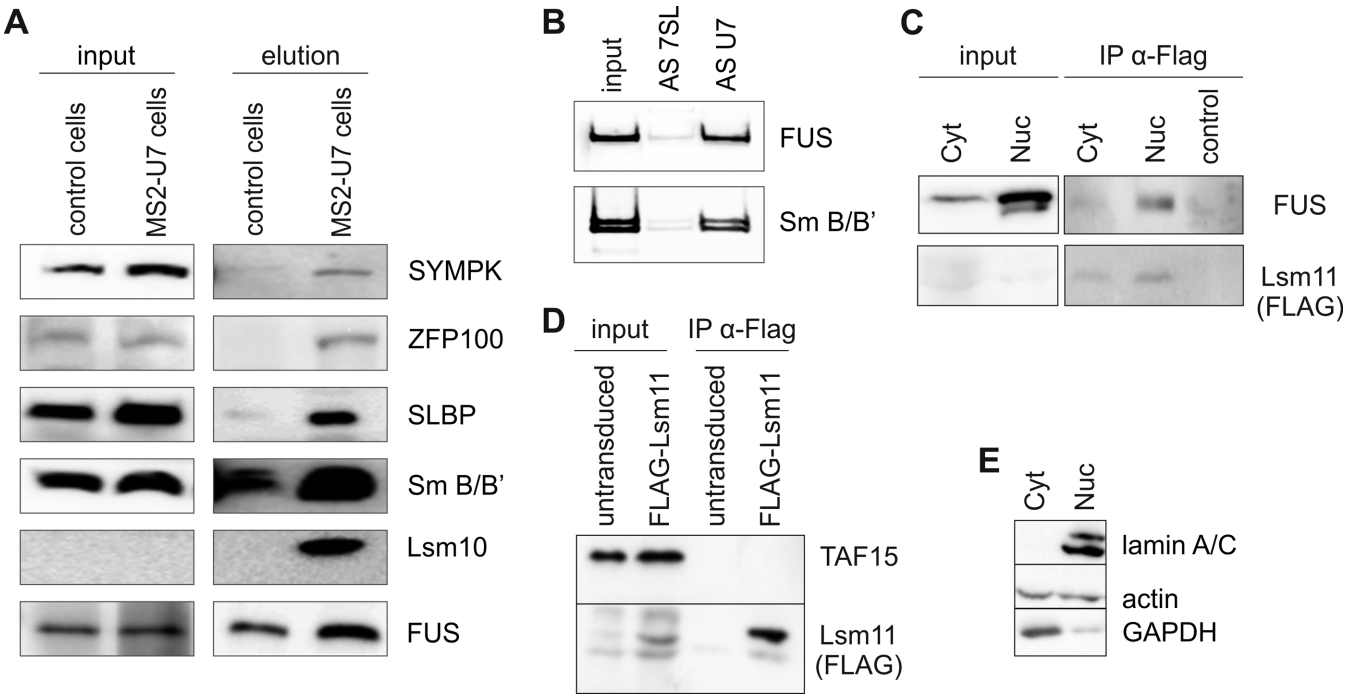

Figure 1. FUS interacts with the U7 snRNP. **(A)** Enrichment of FUS after U7 snRNP affinity purification based on 1x MS2-tagged U7 snRNA (MS2-U7). Western blots confirm the presence of FUS and selected proteins involved in histone RNA processing in the affinity-purified material from MS2-U7 cells. Note that FUS from cells not transduced with the MS2-U7 vector (control cells) also binds weakly to the beads loaded with MBP-MS2. **(B)** Enrichment of FUS after U7 snRNP affinity purification with a biotinylated antisense oligonucleotide (AS U7) complementary to U7 snRNA. An antisense oligonucleotide complementary to 7SL RNA (AS 7SL) was used as negative control. Western blots confirm the presence of FUS and SmB/B' in the AS-U7 enriched fraction. Input: 10% of the used material. **(C)** Co-precipitation of FUS with Lsm11. Western blots confirm the presence of FUS and FLAG-Lsm11 in the immunoprecipitated fractions from HeLa cells stably transduced with a lentiviral construct expressing FLAG-Lsm11. Cyt, cytoplasmic fraction, Nuc, nuclear fraction, control, nuclear fraction from non-transduced HeLa cells. **(D)** Western blot demonstrating that FLAG-Lsm11 does not interact with TAF15. Nuclear extracts from HeLa cells either transduced with the FLAG-Lsm11 vector or untransduced (as a negative control) were used. IP α-FLAG: immunoprecipitation with anti-FLAG antibody; input: 10% of the used material. The additional bands seen in the anti-FLAG blot of untransduced cells are non-specific cross-reactants. In contrast, the lower band seen in the immunoprecipitate may represent a shorter form of Lsm11, possibly a degradation product. **(E)** The quality of the nucleo-cytoplasmic fractionation was verified using anti-lamin A/C, anti-β-actin and anti-GAPDH antibodies.

also the U7 snRNP:FUS complexes are more concentrated in the nuclear than in the cytoplasmic fraction. As, in two of our MS analyses of U7-enriched fractions, we had also detected TAF15 which belongs to the FET protein family like FUS, we analyzed whether it can also be co-precipitated with FLAG-Lsm11, but this was not the case (Figure 1D). In this experiment we used non-transduced HeLa cells as negative control. Moreover, we validated the nuclear/cytoplasmic fractionation with antibodies against lamin A/C, β-actin and GAPDH (Figure 1E).

As the above experiments had indicated that FUS can be enriched by purification or immunoprecipitation of U7 snRNPs, we wanted to know if the inverse is also true. Thus, HeLa nuclear extracts were incubated with beads coupled to two different anti-FUS antibodies or, as negative control, to an antibody against the V5 tag. RNA isolated from these precipitates was reverse transcribed by a coupled polyadenylation reverse transcription reaction, and the concentrations of U7 and U6 snRNAs as well as those of the 7SL RNA were analyzed by qPCR. About 10% of the total U7 snRNA pool was co-precipitated with FUS antibodies, compared to only 0.4% and 0.1% for U6 and 7SL RNA, respectively (Figure 2). Even though the control immunoprecipitation with the anti-V5 antibody brought down ∼4% of the U7 snRNAs, both FUS-specific antibodies precipitated ∼2.4 times more U7 snRNA. Taken together, these results indicate that FUS interacts with U7 snRNPs *in vivo*.

The FUS-U7 snRNP interaction, but not FUS expression, is cell cycle-regulated

Replication-dependent histone gene expression is tightly cell cycle-regulated. Therefore we asked whether the level of the FUS protein or its interaction with the U7 snRNP are subject to cell cycle regulation. To this end, HeLa cells were arrested in G2/M by blocking for 18 h in nocodazole. After release from the block, the cells were collected every 2 h, and cell synchrony was monitored by flow cytometry of propidium iodide-stained cells. Most of the cells divided synchronously within 2 h of release, entered S phase by 10–12 h after release and completed the next, partly synchronous, mitosis by 18–20 h (Figure 3A). This synchronization was confirmed by detection of cyclin B1 by Western blot (Supplementary Figure S2A). Nuclear and cytoplasmic fractions were then prepared and probed by Western blot for FUS, Lsm11, β-actin (Figure 3B) and lamin A/C (Supplementary Figure S2B). Interestingly, we observed a higher level of Lsm11 in the cytoplasm, whereas FUS appeared to be predominantly nuclear (Figure 3B). Because the analyses

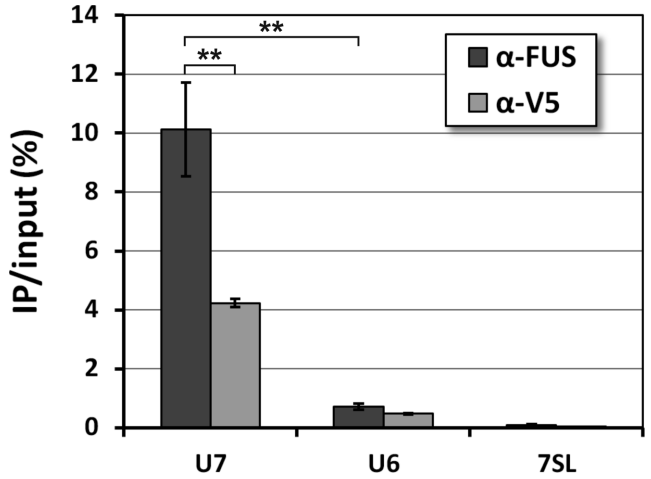

Figure 2. U7 snRNA can be enriched by FUS immunoprecipitation. HeLa nuclear extract was subjected to immunoprecipitation with two different anti-FUS antibodies (dark grey) and one anti-V5 antibody (light grey; negative control), and the levels of U7 and U6 snRNAs as well as those of 7SL RNA were quantitated by RT-qPCR. The amounts detected in the immunprecipitates (IP) are expressed as percent of the input. Error bars indicate standard deviations (SD) of three technical replicates for each antibody (i.e. six and three values for anti-FUS and anti-V5, respectively). *P*-values were calculated using Student's T-test, and statistical significance is represented as follows: $^{**}P \leq 0.01$.

of lamin A/C (Supplementary Figure S2B) and FUS (Figure 3B) had indicated a partial leakage of nuclear content into the cytoplasmic fractions in the earliest time points, the unreliable, but also less relevant, 0 and 2 h points were omitted from the quantitative analyses shown in Figure 3C and D. Based on these analyses, the levels of FUS and Lsm11, and especially the nuclear levels, showed only minor fluctuations but no pronounced cell cycle regulation.

We then decided to analyze the FUS-U7 snRNP interaction in synchronized cells. For this purpose, we used HEK 293T cells stably overexpressing FLAG-FUS or FLAG-EBFP (used as negative control). The cells were synchronized by nocodazole block and brought to G1, S or G2 phase after the release (Figure 4A). Protein extracts were isolated and incubated with anti-FLAG antibody-coupled magnetic beads. RNA isolated from the beads was subjected to reverse transcription by a coupled polyadenylation RT reaction using an anchored oligo(dT) primer. U7 snRNA and histone H3c mRNA were then quantified by qPCR. Most U7 snRNA was precipitated with FUS in S phase samples (Figure 4B). Interestingly, H3c mRNA was also enriched by FLAG-FUS immunoprecipitation, and, similarly to U7 snRNA, the enrichment was most pronounced in S phase (Figure 4C). A similar S phase-specific increase in co-precipitation could also be observed for H2Ac, H2Bc, H2Bj, H3e and H4l mRNAs, but not for the replication-independent H2A.Z mRNA (Figure 4D).

FUS affects the expression of U7 snRNA and replication-dependent histone RNAs

The S phase-specific interaction of FUS with the U7 snRNP and replication-dependent histone gene transcripts suggested that FUS may play a role in histone RNA 3′ end processing. To study this possibility, we measured U7 snRNA levels and the processing of histone mRNAs in HeLa cells depleted of or overexpressing FUS. The depletion was achieved by expressing a shRNA targeting FUS from a doxycycline-inducible lentiviral vector. A vector encoding a shRNA against T-cell receptor β (TCRβ, which is not expressed in these cells) was used as control. Preliminary experiments showed that such a depletion has minimal effects on cell cycle progression. The FUS-depleted cells showed a slight delay in the transition from G1 to S phase compared to the two control cells (shFUS cells without doxycycline induction and shTCRβ cells with doxycycline; Supplementary Figure S3A). Proliferation rates were close to normal for 4 days and then started to decrease (Supplementary Figure S3B). After 7 days of doxycycline induction, the FUS protein was reduced to ∼15% of uninduced levels (Figure 5A). Importantly, FUS depletion caused a ∼50% reduction in U7 snRNA levels (Figure 5B). This is consistent with previous findings that FUS interacts with SMN and may be involved in snRNP biogenesis (68,69). As a second system to study FUS effects, we used the previously described HEK 293T cells expressing FLAG-tagged FUS and the similarly produced FLAG-EFBP cells as controls. The overexpression of FUS in the FLAG-FUS cells was ∼50% over the normal level (Figure 5A). These cells showed a ∼35% increase in U7 snRNA levels but this effect was statistically not significant.

Based on these changes in U7 snRNA levels, we wanted to know if histone RNA 3′ end processing is affected. For this we measured the steady state levels of total and unprocessed transcripts for various representatives of replication-dependent histone genes by an RT-qPCR approach with primer sets targeting either the mRNA body or a region downstream of the processing site and used the replication-independent H2A.Z gene as control (Figure 5D). As introduced in previous papers (22,25,70), the fraction of correctly processed RNA was defined as apparent processing efficiency. 'Apparent' because the levels of correctly processed to unprocessed RNAs at steady state are not only influenced by processing but also by the turnover rates of the precursor and its product which are likely to be different. In the FUS-depleted cells, the apparent processing efficiency was reduced for all five analyzed replication-dependent histone genes, but not for the replication-independent H2A.Z gene (Figure 5E). In the FLAG-FUS overexpressing cells, the H2Ac and H2Bc genes showed an increase in the fraction of correctly processed transcripts (Figure 5F). For the H3e gene, the increase of 43% was not statistically significant.

A more differentiated picture emerged, when we plotted the amounts of total histone transcripts and extended ones separately (Supplementary Figure S4A). Four genes that had shown a reduction in the fraction of correctly processed transcripts in the FUS-depleted cells showed reduced levels of total transcripts, whereas the read-through transcripts were slightly increased or unchanged. For the H2Ac gene, both the total and read-through transcripts were elevated. In the FUS overexpressing cells, the H2Ac and H2Bc genes showed close to normal levels of total transcripts but reduced levels of extended ones. In contrast, for the H3e gene both types of transcripts were more abundant. The reasons

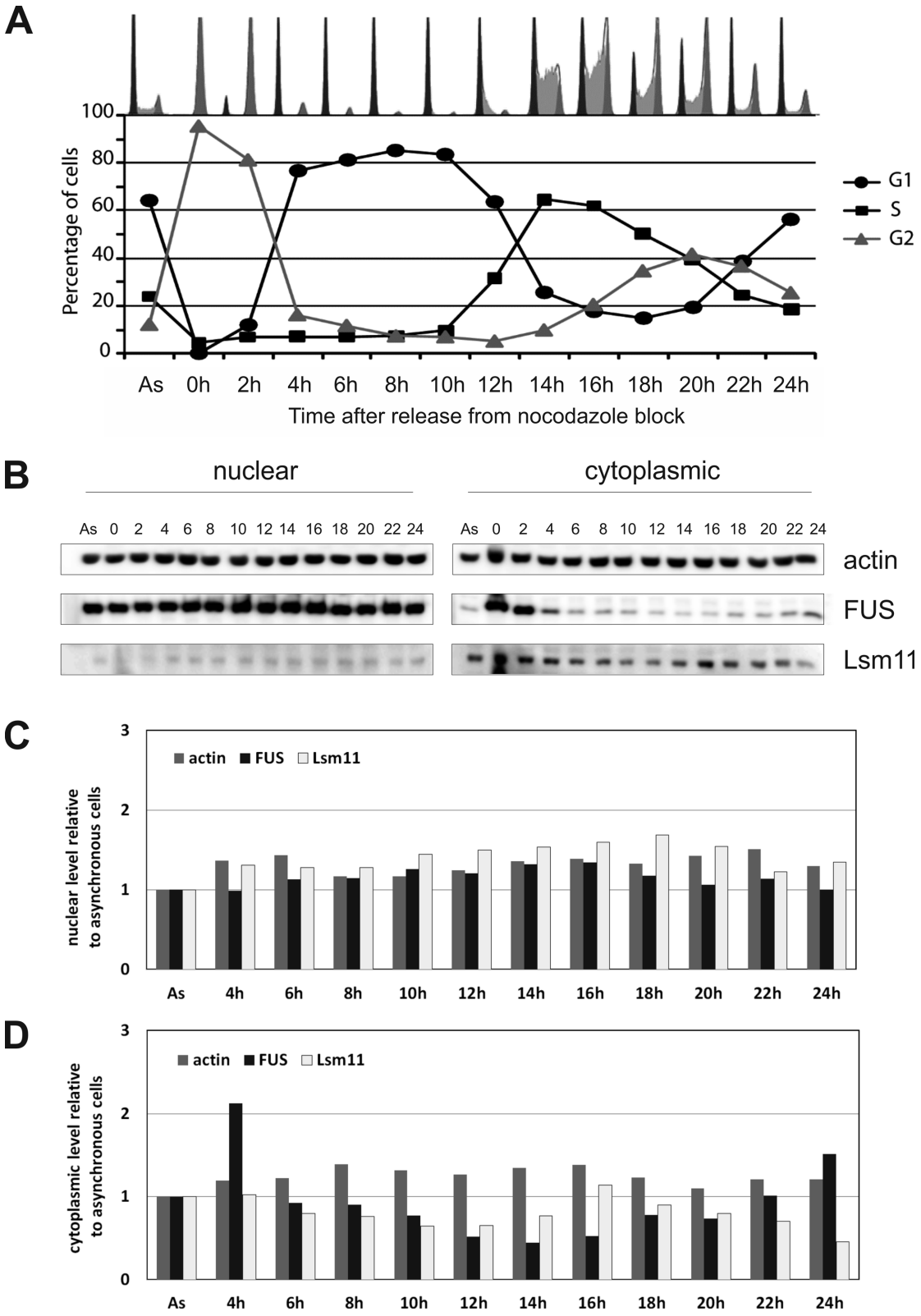

Figure 3. Nuclear and cytoplasmic FUS levels during the cell cycle of synchronized HeLa cells. **(A)** Cells synchronized by nocodazole block were analyzed by flow cytometry of propidium iodide-stained cells. Profiles of individual time points after release of the block are shown at the top and the percentages of cells in the indicated cell cycle phases are plotted below. Note that a DNA content typical for G2 means that the cells are in either G2 or M phase. **(B)** Western blots using anti-β-actin, anti-FUS and anti-Lsm11 antibodies to analyze the expression levels of these proteins in nuclear (left) and cytoplasmic (right) fractions isolated at the various time points. The levels of FUS, Lsm11 and β-actin were quantitated and normalized to those observed in asynchronously dividing cells in both the nuclear **(C)** and cytoplasmic **(D)** fractions. Due to leakage of nuclear content into the cytoplasmic fractions (possibly due to nuclear envelope breakdown during mitosis), the time points 0 and 2 h after nocodazole release were omitted from these quantitations. As, asynchronously proliferating cells.

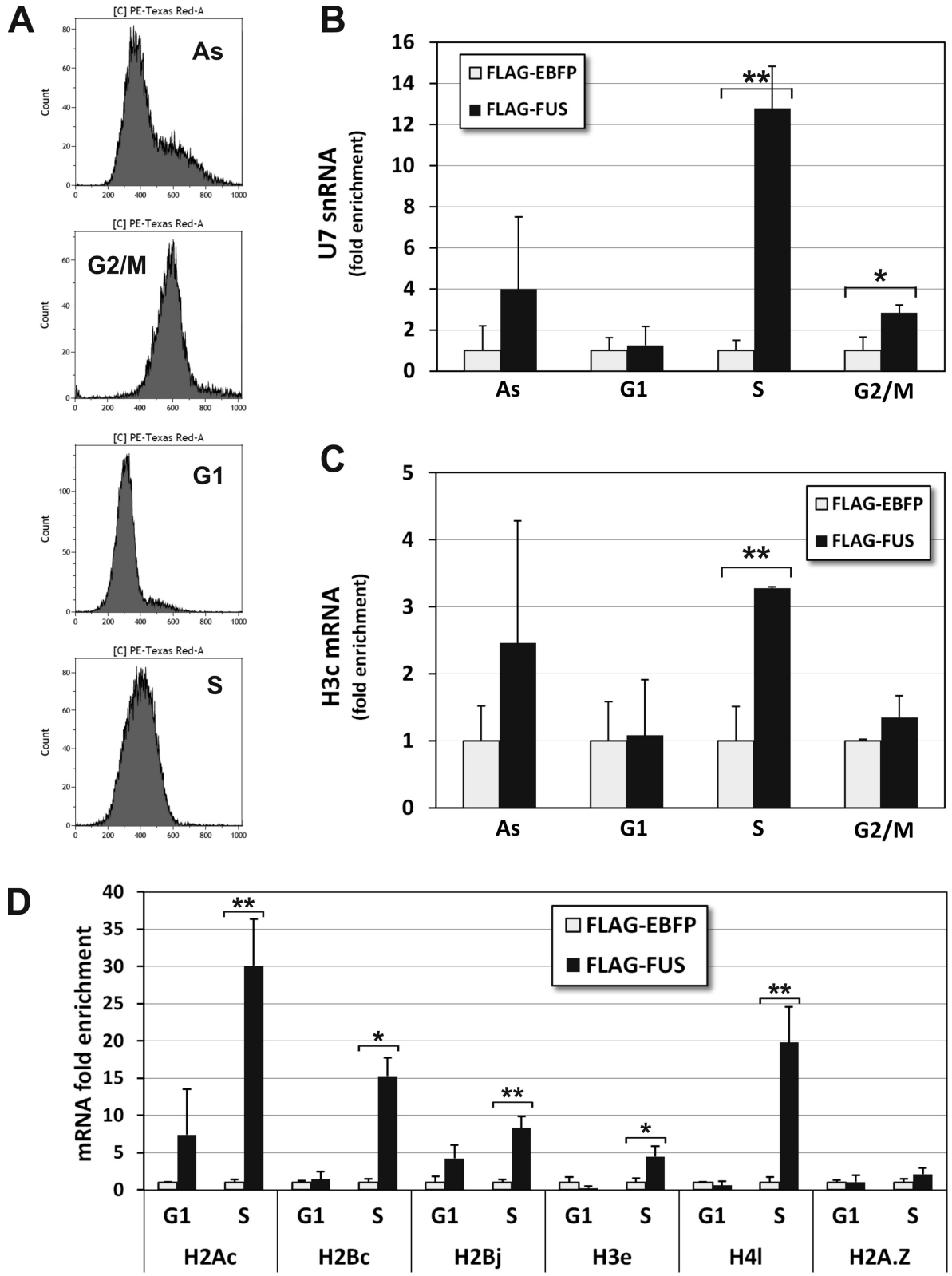

Figure 4. U7 snRNA and replication-dependent histone RNAs can be co-precipitated with FUS. **(A)** Cytofluorometry profiles of propidium iodide-stained, asynchronously dividing (As) and synchronized HEK 293T cells stably overexpressing FLAG-FUS or FLAG-EBFP. The cells were synchronized by nocodazole block followed by release for 2 (G2/M), 5 (G1) and 15 h (S). Nuclear extracts were subjected to immunoprecipitation with anti-FLAG antibody. The amounts of U7 snRNA **(B)** and histone H3c mRNA **(C)** in FLAG immunoprecipitates relative to the input were measured by RT-qPCR and normalized for FLAG-EBFP. **(D)** Similar immunoprecipitation and RT-qPCR analyses of H2Ac, H2Bc, H2Bj, H3e, H4l mRNAs as well as the replication-independent H2A.Z mRNA in nuclear extracts from G1 and S phase cells. Error bars represent SD of three biological replicates. *P*-values were calculated using Student's T-test, and statistical significance is represented as follows: $*P \leq 0.05$; $**P \leq 0.01$.

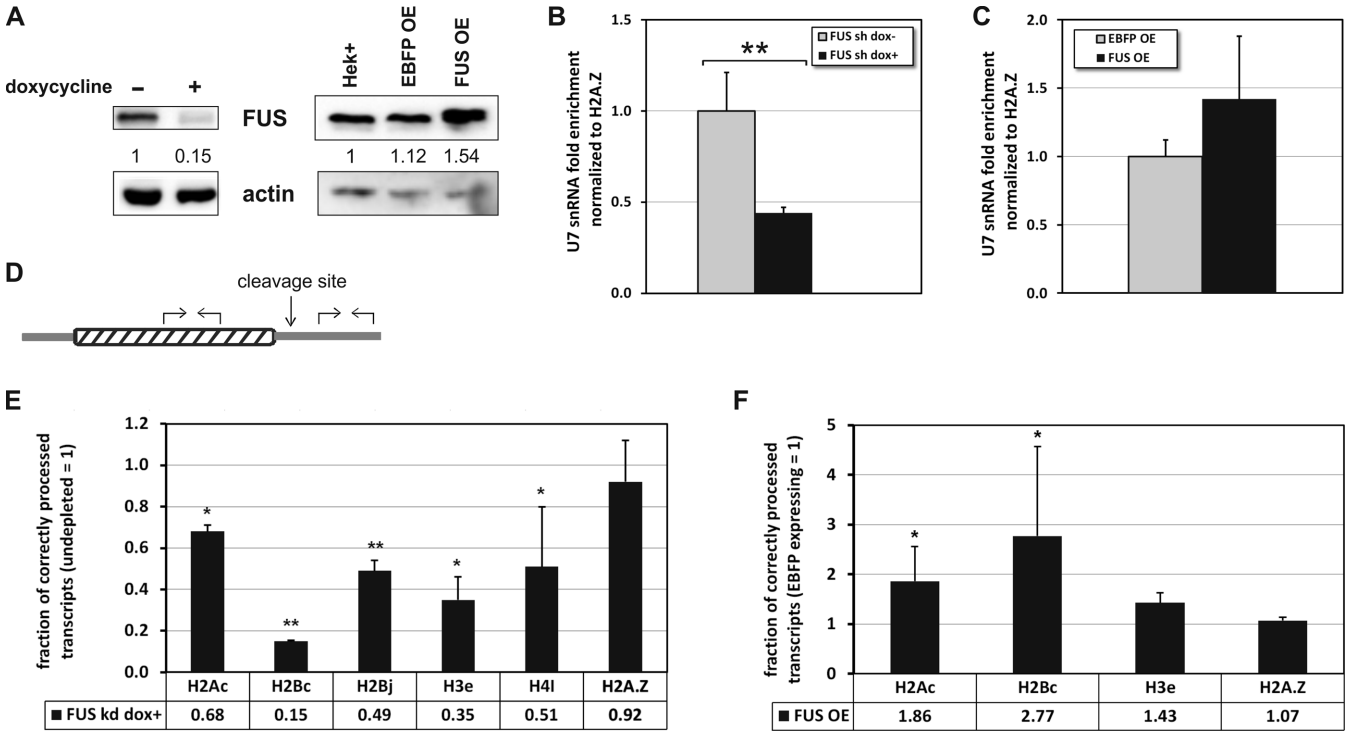

Figure 5. Effects of FUS depletion and overexpression on U7 snRNA and replication-dependent histone gene expression. **(A)** Extent of FUS depletion after 7 days of doxycycline induction of shFUS-Krab HeLa cells (left) and of FUS overproduction in FLAG-FUS expressing HEK 293T cells (right). The panels show Western blots probed for FUS (upper panels) and β-actin (lower panels, loading control) with relative amounts of FUS protein listed in between. **(B)** U7 snRNA levels in FUS-depleted HeLa cells determined by RT-qPCR. The level of U7 snRNA in shFUS-Krab cells not induced with doxycycline was used as reference (relative level = 1). **(C)** U7 snRNA levels in FLAG-FUS overexpressing HEK 293T cells. The level of U7 snRNA in FLAG-EBFP expressing cells was used as reference (relative level = 1). **(D)** Location of primer pairs used in RT-qPCR to determine the apparent processing efficiency of various histone genes (i.e. the ratio of correctly processed to unprocessed RNA at steady state which is influenced not only by processing but also by turnover of the precursor and its product). For each gene, one set was located in the open reading frame to detect total (correctly processed plus extended) histone transcripts. The second primer pair was located downstream of the processing site to detect extended transcripts. **(E)** Fraction of correctly cleaved histone transcripts in FUS-depleted (FUS kd dox+) HeLa cells measured by RT-qPCR. The values have been normalized to those of cells not treated with doxycycline. **(F)** Fraction of correctly cleaved histone transcripts in FLAG-FUS overexpressing HEK 293T cells (FUS OE) cells. The values have been normalized to those of cells expressing FLAG-EBFP. Note that H2A.Z is a replication-independent histone gene that was used as a reference. Error bars in B C, E and F represent SD of three biological replicates. *P*-values were calculated using Student's T-test, and the statistical significance is represented as follows: $*P \leq 0.05$; $**P \leq 0.01$.

for these different responses to FUS depletion and overexpression are not clear, but similar gene-specific responses to an interference in histone RNA processing have previously been observed by Johnsen's laboratory (71). Nevertheless, the net result was a reduced apparent processing efficiency in FUS-depleted cells and an improvement in the FUS overexpressing cells. However the data also suggested that FUS may exert effects both on the transcription and on the processing of replication-dependent histone transcripts.

To visualize the histone read-through transcripts, we amplified H2Be by RT-PCR from total RNA of shFUS cells treated or not treated with doxycycline. The levels of GAPDH and H2A.Z transcripts used as controls were, if anything, reduced by the FUS depletion (Supplementary Figure S4C). In contrast, the extended transcripts of the H2Be gene could be shown to increase upon FUS depletion. This was in agreement with the results obtained above for various replication-dependent histone genes by RT-qPCR and indicated a defect in histone RNA 3′ end processing.

Taken together these results support the idea that FUS influences the expression of several if not all replication-dependent histone genes. It appears to act as a positive regulator of correctly processed transcripts.

FUS interacts with NPAT and hnRNP UL1 in a cell cycle-regulated manner

We then wanted to study if FUS interacts with other factors involved in replication-dependent histone gene expression besides already established U7 components or well characterized processing factors as shown above. In particular, we were interested to see if NPAT or hnRNP UL1 may interact with FUS. NPAT is a histone-specific transcription factor involved in the transcriptional control of replication-dependent histone gene expression during the cell cycle (3,72). Moreover it is an important component of histone locus bodies, subnuclear areas containing the clusters of replication-dependent histone genes and various factors involved in histone gene expression (3). Depletion of NPAT has also been shown to cause a defect in histone RNA 3′ end processing (72,73). In contrast, hnRNP UL1 has been shown to interact with U7 snRNPs and to be involved in a special regulatory activity of the U7 snRNP out-

side of the S phase. While the U7 snRNP is an essential factor for 3′ end processing during S phase, it can, together with hnRNP UL1, cause a transcriptional repression of the replication-dependent histone genes in the other cell cycle phases (27).

In an initial experiment, HeLa nuclear extract was subjected to immunoprecipitation with α-FUS antibodies. As shown in Figure 6A, a significant fraction of NPAT and hnRNP UL1 could be co-immunoprecipitated with FUS. Moreover, as expected, based on its interaction with the U7 snRNP, a small fraction of the general snRNP protein SmB/B' was also co-precipitated.

To analyze these interaction in more detail, we bacterially produced MBP-tagged recombinant FUS proteins. Details of the purification are shown in Supplementary Figure S5. The full-length (FL) protein could only be purified in small amounts, but a deletion mutant lacking the first 165 amino acids (ΔNT) was well expressed in *E. coli* (Figure 6B). When similar amounts of the two proteins bound to amylose resin were used for an affinity purification of HEK 293T nuclear extract and the recombinant proteins with their bound interaction partners were eluted with TEV protease and analyzed by Western blotting, we found that both proteins associated with UL1, ZFP100 and SmB/B' (Figure 6C). However, the amount of UL1 recovered by FUS ΔNT was lower than with FL FUS. Because of the poor yields of recombinant FL FUS, we nevertheless decided to use FUS ΔNT for the subsequent experiments.

To analyze whether the interactions of FUS with NPAT and hnRNP UL1 are cell cycle-regulated, similar binding experiments with recombinant FUS ΔNT were repeated with nuclear extracts isolated from cells synchronized in the G1, S and G2 phases of the cell cycle. As shown in Figure 6D, the binding of NPAT was most prominent with extract from S phase-synchronized cells, while the interaction with hnRNP UL1 was stronger in the other cell cycle phases. In contrast, the binding of ZFP100 to FUS showed no obvious cell cycle dependence. As a control for the specificity of this assay, we tested whether a MBP-tagged bacterially produced version of the related FET protein TAF15 (Supplementary Figure S6A) can interact with UL1. As shown in Supplementary Figure S6B, TAF15 did not bind to UL1 from extracts of either asynchronously dividing HEK 293T cells or cells synchronized in G1 or S phase, whereas the binding to FUS ΔNT could be confirmed.

Taken together, these experiments indicate that FUS interacts with NPAT and hnRNP UL1. Interestingly, it does so predominantly in those phases of the cell cycle in which these proteins exert their effects on histone gene expression, i.e. S phase for NPAT and non-S for hnRNP UL1.

FUS interacts with promoters of replication-dependent histone genes and enhances their activity

As FUS was found to influence the level of histone mRNAs and to be associated with factors such as NPAT and hnRNP UL1 involved in the expression of replication-dependent histone genes, we wanted to see whether it can associate with histone gene regions. For this purpose, we performed a chromatin immunoprecipitation (ChIP) experiment with anti-FLAG antibody in HEK 293T cells stably overexpressing FLAG-FUS, FLAG-EBFP (negative control) or no FLAG-tagged protein. The experiment was performed with cells synchronized either in G1 or S phase. Different primers were used to amplify the promoter regions, open reading frames and 3′ UTR regions of three replication-dependent histone genes. After subtraction of the signals of normal HEK 293T cells, the fold enrichment of precipitated material from FLAG-FUS cells compared to FLAG-EBFP cells was calculated. The results shown for H2Bj in Figure 7A and for H2Ac and H4j in Supplementary Figure S7A and B indicated that FUS interacts predominantly with the promoter regions of these three histone genes and that this interaction is much stronger in the S phase than in the G1 phase. In contrast we observed no significant interaction with the promoter region of the replication-independent H2A.Z histone gene, be it in G1 or in S phase (Supplementary Figure S7C).

Based on these results, we performed a similar ChIP experiment with an antibody against RNA polymerase II (RNAP2). As shown in Figure 7B, we observed an enrichment of RNAP2 at the histone H2Bj gene promoter, open reading frame and 3′ UTR region in FUS overexpressing cells compared to FLAG-EBFP expressing cells in S phase. This indicated that FLAG-FUS overexpression stimulates the presence of RNAP2 on the histone H2Bj gene. In the same experiment, the recruitment of RNAP2 was significantly inhibited in G1 phase. Inversely, FUS depletion inhibited RNAP2 loading in all three segments of the H2Bj gene in S phase cells, but caused an enhanced recruitment in G1 phase cells (Figure 7C). This indicates that FUS can regulate RNAP2 recruitment to histone genes during the cell cycle.

To see whether this differential recruitment of RNAP2 to histone genes is reflected by changes in the activity of the histone promoters, we cloned several histone promoters upstream of a GFP reporter gene and tested these constructs after transient transfection in HeLa cells which were subjected to a FUS depletion (see Materials and Methods). A cotransfected β-globin expression plasmid served as normalizer and internal control for differences in transfection efficiency. As shown in Figure 8, the activity of four of the five analyzed promoters is significantly impaired by the FUS depletion. Only the H4n promoter shows an activity close to that of undepleted cells.

The effects of our various manipulations of FUS protein levels on the apparent histone RNA 3′ end processing, gene loading by RNAP2 and histone promoter activity raised the question whether these changes might be reflected in histone protein levels. Therefore we assessed the levels of various histone proteins in cells with FUS overexpression or depletion (Supplementary Figure S8). Surprisingly, the histone protein levels were substantially unchanged. Possible reasons for this paradoxical behavior will be discussed below.

DISCUSSION

The expression of the replication-dependent histone genes is strongly up-regulated during the G1/S phase transition to prepare the cells for the replication of their genome. The newly synthetized DNA has to interact with histone pro-

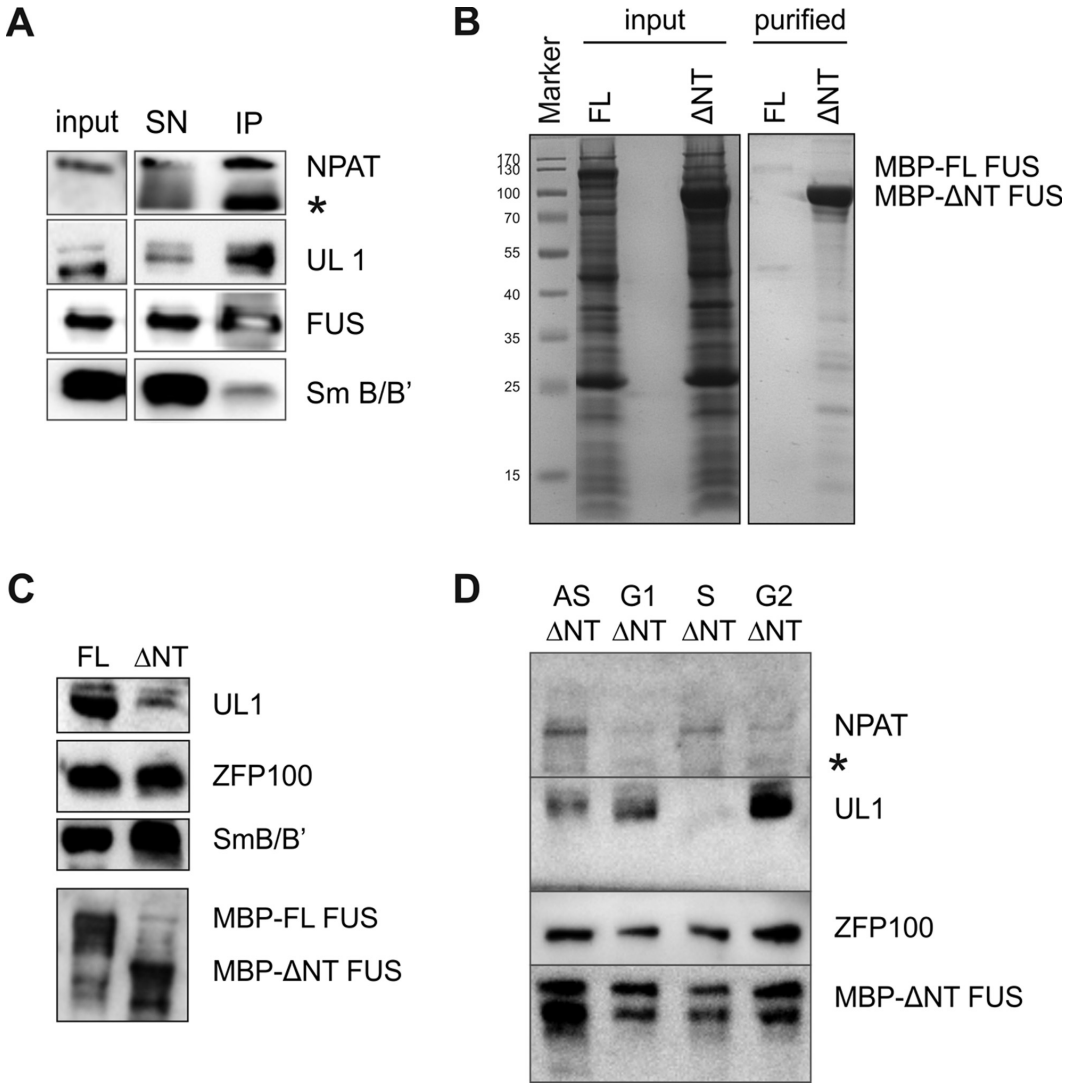

Figure 6. Interactions of FUS with NPAT and hnRNP UL1. **(A)** Western blot demonstrating the interaction of FUS with NPAT, hnRNP UL1 and SmB/B' after immunoprecipitation of HeLa nuclear extract with anti-FUS antibody. SN: supernatant; IP: immunoprecipitation. **(B)** Recombinant full-length FUS (FL) and an N-terminal deletion of amino acids 1-165 (ΔNT) were overexpressed as MBP fusions in bacteria (input) and purified using amylose beads (purified). **(C)** Interaction of these recombinant FUS proteins (FL and ΔNT) present in roughly equal amounts with hnRNP UL1, ZFP100 and SmB/B'. **(D)** Cell cycle-dependence of the interactions of FUS (ΔNT) with NPAT and hnRNP UL1. AS, asynchronously proliferating cells; S, G1, G2, cells in S, G1, G2 phase, respectively; *: unspecific signal.

teins to form chromatin and to maintain genome stability. Then, at the end of S phase, the availability of histones must be reduced because an excess could be harmful to the cells. This regulation has to ensure that the expression of the ∼50 genes encoding the different histone proteins in mammals (74) is tightly coordinated. To do so, it operates at three levels: transcription, mRNA maturation and transcript stability (2). At all these steps, specific factors are involved, some of which are cell cycle-regulated themselves.

NPAT and hnRNP UL1 are important components regulating the transcription of histone genes. NPAT activates the transcription of all the replication-dependent histone genes by interacting with upstream promoter elements and with other transcription factors that are specific for different histone subtypes (e.g. OCA-S or HINF-P which are specific for H2B and H4 gene promoters, respectively) (75,76). In contrast, hnRNP UL1 has been found to associate with the U7 snRNP and to repress transcription under cell cycle arrest conditions (27). If one assumes that this latter process also operates in a normal cell cycle, then the transcription of the replication-dependent histone genes would be regulated both positively (in S phase, by NPAT) and negatively (in the other phases of the cell cycle, by hnRNP UL1 in conjunction with the U7 snRNP). Together, these mechanisms result in a ∼5-fold regulation of histone gene transcription over the cell cycle (2).

The efficiency of histone RNA 3′ end processing is upregulated ∼8-fold during the G1/S phase transition (2). This reaction, which is unique to the replication-dependent histone genes, is mediated by the U7 snRNP in cooperation with several other factors (4–6). Two of these are cell cycle-regulated, i.e. SLBP (26) and the CstF64 component of the

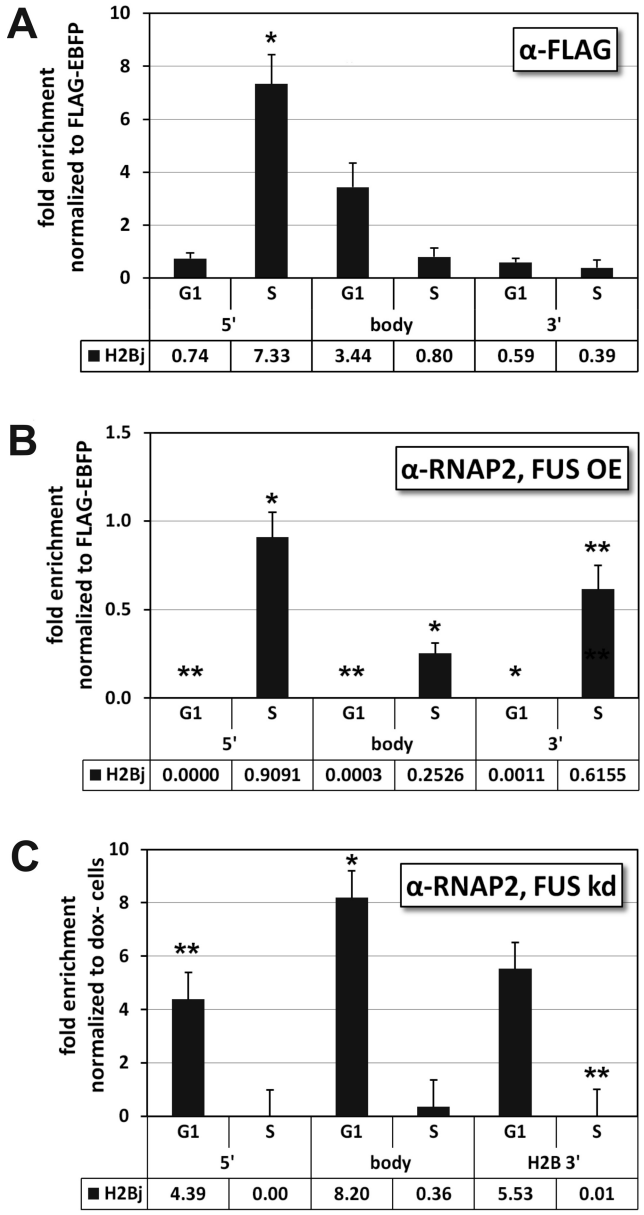

Figure 7. FUS binds to promoter regions of replication-dependent histone genes during S phase and enhances the binding of RNA polymerase II to histone genes. **(A)** ChIP assays using anti-FLAG antibodies and showing an S phase-specific enrichment of FLAG-FUS in the promoter region of the H2Bj gene. FLAG-EBFP overexpressing cells were used as negative control. Different qPCR reactions were performed to detect the promoter region, open reading frame and 3′ UTR region. Similar analyses for additional genes are shown in Supplementary Figure S7. **(B)** ChIP experiment performed with anti-RNAP2 antibody showing that FLAG-FUS overexpression stimulates the association of RNAP2 with the H2Bj gene in S phase and inhibits its binding in G1 phase. FLAG-EBFP overexpressing cells were used as negative control. **(C)** ChIP experiment performed with anti-RNAP2 antibody showing that FUS depletion reduces the association of RNAP2 with the H2Bj gene in S phase and allows a stronger recruitment in G1 phase. Cells without FUS depletion by doxycycline treatment were used as negative control. Error bars represent the SD of three biological replicates. *P*-values were calculated using Student's T-test, and the statistical significance was represented as follows: $*P \leq 0.05$; $**P \leq 0.01$.

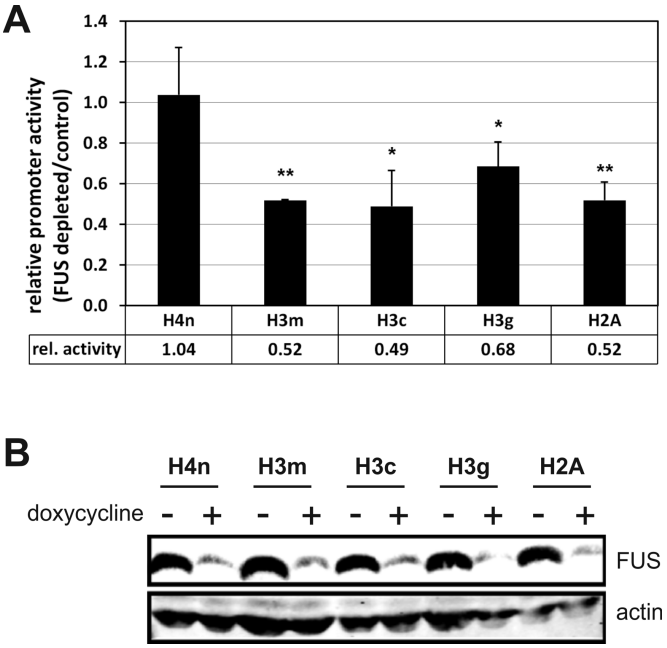

Figure 8. Effect of FUS-depletion on histone promoter reporter assays. **(A)** The levels of EGFP reporter mRNA expressed under the indicated histone promoters were analyzed in FUS-depleted HeLa cells relative to cells not treated with doxycycline and normalized to the mRNA levels of a co-transfected β-globin gene. Error bars indicate standard deviations (SD) of four biological replicates. *P*-values were calculated using Student's T-test, and statistical significance was represented as follows: $*P \leq 0.05$; $**P \leq 0.01$. **(B)** Extent of FUS depletion assessed by Western blot. β-actin is used as loading control.

HLF (1,25). Additionally, SLBP bound to the conserved 3′-terminal stem-loop facilitates the export of the mature histone mRNAs to the cytoplasm and enhances their translation and stability. The phosphorylation and subsequent degradation of SLBP at the end of S phase is also responsible for a rapid destabilization of all replication-dependent histone mRNAs that results in their clearance from the cell (26).

Our results reveal that FUS/TLS plays an important role in the coordination and control of replication-dependent histone gene expression. Notably, FUS interacts with the U7 snRNP/U7 snRNA as well as with replication-dependent histone gene transcripts and does so predominantly during the S phase of the cell cycle (Figures 1, 2 and 4). Moreover, FUS depletion and overexpression both affect the ratio of correctly processed to read-through transcripts for several replication-dependent histone genes (Figure 5). Taken together, these findings indicate that FUS acts as a positive effector of histone RNA 3′ end processing. Additionally, the interactions of FUS with NPAT and hnRNP UL1 (Figure 6) indicate an involvement in histone gene transcription. As we found that FUS:NPAT and FUS:hnRNP UL1 complexes are prominent in different phases of the cell cycle, FUS may actually play a role in switching between the NPAT-mediated transcriptional activation during S phase and the hnRNP UL1-mediated transcriptional repression in the other phases of the cell cycle. A role for FUS in histone gene transcription is further corroborated

by our finding that FUS binds to histone gene promoters, predominantly during S phase, and that its overexpression stimulates the association of RNA polymerase II (RNAP2) with the replication-dependent histone gene regions (Figure 7). In the same experiment a significant inhibition of RNAP2 association with histone gene promoters was observed in G1 phase cells. Moreover, FUS overexpression had the opposite effect on the recruitment of RNAP2 to the replication-dependent histone genes (Figure 7), and we could demonstrate that FUS regulates the activity of histone promoters (Figure 8). Thus, FUS appears to play a role as a linking factor that enhances the transcription and correct 3′ end processing of the replication-dependent histone gene transcripts by interacting with the U7 snRNP and other important regulatory factors. However, outside of the S phase it may act as negative regulator in complex with hnRNP UL1.

Despite the fact that there have been several searches for FUS interactors (e.g. (43,68,77)), connections with components of the histone gene expression machinery have not yet been reported. Possibly, if such interactions have been found in previous studies, they may have been neglected because they occurred at a very low level. What brought FUS to our attention was its identification in strongly enriched U7 snRNP preparations. Moreover, we have shown that these interactions occur in certain phases of the cell cycle which means that they might easily be overlooked in samples from asynchronously dividing cells.

How FUS binds to NPAT, hnRNP UL1 and the U7 snRNP and how it links these factors with each other will have to be elucidated in more detail. In particular it is not yet clear if all the effects on histone gene expression that we have documented are caused by changing U7 levels or if FUS also acts on histone gene expression (e.g. at the transcriptional level) independently of the U7 snRNP. A likely scenario is that FUS regulates the accessibility of the U7 snRNP to different partners during the cell cycle. It was previously demonstrated that hnRNP UL1 interacts with the U7 snRNP (27), and we have shown here that FUS is associated with hnRNP UL1 predominantly in G2 and G1 and with the U7 snRNP and with histone transcripts predominantly during S phase. In this scenario, FUS would be important for histone RNA processing in S phase (as demonstrated in this paper), but might also repress histone gene transcription outside of S phase (which remains to be analyzed).

Another function of FUS in histone gene expression appears to be to stimulate histone gene transcription in S phase and possibly to coordinate transcription with RNA 3′ end processing. Its interaction with NPAT, which is most prominent during S phase, is most likely responsible for the observed stimulatory effect on the presence of RNAP2 on histone gene loci and the activation of histone gene promoters. There are precedents for such a transcriptional function of FUS. In particular, it has been shown to associate directly with RNAP2 and with the general transcription factor TFIID (37) and to participate in the recognition of promoters by binding to certain transcriptional activators (38,39).

Additionally, the interaction between FUS and NPAT could play a role in coupling histone gene transcription and 3′ end processing. In contrast to polyadenylated mRNAs where a coupling between transcription and cleavage/polyadenylation is well established (78), the evidence for a similar mechanism acting on the replication-dependent histone genes is scarce. In an *in vitro* transcription system from *Drosophila*, Adamson and Price did not observe a pronounced coupling (79). Evidence from the Manley lab that the phosphorylation of threonine 4 (Thr4) in the C-terminal domain (CTD) of RNAP2 is required for histone RNA 3′ end processing (80) strongly stimulated the concept of coupling for histone genes, but the Thr4 phosphorylated form of RNAP2 was then also found to be associated with other genes and was suggested to play a more general role in transcriptional elongation (81,82). However, the findings that NPAT can interact with Lsm11 via FLASH and that FLASH interacts with histone gene promoters (19) and that NPAT depletion affects the efficiency of histone RNA 3′ end processing (73) suggested that the transcription and processing of replication-dependent histone RNAs are somehow linked through NPAT, FLASH and the U7 snRNP. In such a scheme, FUS could play an important role, as we have shown it to interact with NPAT and the U7 snRNP and to promote RNAP2 occupancy on histone genes during S phase. More specifically, FUS, in concert with NPAT and other histone-specific and general transcription factors, might enhance both the presence and activity of RNAP2 on histone genes and the loading of the CTD domain with the U7 snRNP or with other histone RNA processing factors.

Despite the fact that histone gene transcription and 3′ end processing were affected by our experimental manipulations of the FUS level, the levels of histone proteins seemed to be unaffected (Supplementary Figure S8). A likely explanation for this paradoxical result is that too high or too low histone protein levels should be toxic to the cells. Thus, a cell should either adapt its proliferation to the available histone levels or die. Our depletion and overexpression conditions are not so extreme that an adaptation is not possible. In fact, the cell cycle and proliferation assays shown in Supplementary Figure S3 indicate that this is occurring in our system in the sense that proliferation rates appear to be adapted to the amount of FUS present.

As expected for a factor that has many other functions, the levels of the FUS protein are not regulated during the cell cycle (Figure 3). However, as mentioned, several of its interactions with components of the histone gene expression machinery are specific for certain phases of the cell cycle. This raises the question how these interactions may be regulated. Obvious and mutually not exclusive possibilities are that certain components of these complexes may either be cell cycle-regulated themselves or subject to post-translational modifications which alter the assembly, stability or the turnover of the complexes. For example, the level of NPAT protein has been shown to peak at the G1/S boundary, remain high in mid-S phase and then to decrease (83,84). Moreover, NPAT promotes S phase entry, and this effect is enhanced by the cyclin E–CDK2 kinase that selectively phosphorylates NPAT at the G1/S border at nuclear foci related to Cajal bodies. This phosphorylation also stimulates NPAT-mediated transcriptional activation

of replication-dependent histone genes (3,72,84–86). As already mentioned, the phosphorylation of the RNAP2 CTD on Thr4 may also play a role in histone RNA 3′ end processing (80). Last but not least, FUS has also been shown to influence the phosphorylation status of the RNAP2. It binds to the CTD and inhibits premature Ser2 hyperphosphorylation of this domain (86). However, to fully elucidate how the various interactions of FUS with the histone gene expression machinery are regulated will be a challenging task for future investigations.

SUPPLEMENTARY DATA

Supplementary Data are available at NAR Online.

ACKNOWLEDGEMENTS

We thank Assad Alhaboub for help in cell synchronization, primer extension and gradient fractionation experiments, Agata Stepien for technical help and Michal Taube for providing TEV protease. We also thank Prof. Oliver Mühlemann for kindly providing lab space to M.D.R.

FUNDING

Polish Science Centre [UMO-2012/05/B/NZ2/00826 to K.D.R.]; KNOW RNA Research Centre in Poznan [01/KNOW2/2014 to A.J., Z.S-K., K.D.R, A.B.]; SCIEX-NMS^{ch} [10.224 to K.D.R. and D.S.]; Swiss National Science Foundation [31003A_120064, 31003A_135644, 31003A_153199, NCCR RNA to D.S.]; HOLCIM Stiftung zur Förderung der wissenschaftlichen Fortbildung and the NOMIS foundation [to M.D.R.]. Fund for open access charge: Swiss National Science Foundation and Kanton Bern and Adam Mickiewicz University, Poznan, Poland.
Conflict of interest statement. None declared.

REFERENCES

1. Lüscher,B. and Schümperli,D. (1987) RNA 3′ processing regulates histone mRNA levels in a mammalian cell cycle mutant. A processing factor becomes limiting in G1-arrested cells. *EMBO J.*, **6**, 1721–1726.
2. Harris,M.E., Böhni,R., Schneiderman,M.H., Ramamurthy,L., Schümperli,D. and Marzluff,W.F. (1991) Regulation of histone mRNA in the unperturbed cell cycle: Evidence suggesting control at two posttranscriptional steps. *Mol. Cell. Biol.*, **11**, 2416–2424.
3. Ma,T., Van Tine,B.A., Wei,Y., Garrett,M.D., Nelson,D., Adams,P.D., Wang,J., Qin,J., Chow,L.T. and Harper,J.W. (2000) Cell cycle-regulated phosphorylation of p220(NPAT) by cyclin E/Cdk2 in Cajal bodies promotes histone gene transcription. *Genes Dev.*, **14**, 2298–2313.
4. Müller,B. and Schümperli,D. (1997) The U7 snRNP and the hairpin binding protein: Key players in histone mRNA metabolism. *Semin. Cell Dev. Biol.*, **8**, 567–576.
5. Dominski,Z. and Marzluff,W.F. (2007) Formation of the 3′ end of histone mRNA: Getting closer to the end. *Gene*, **396**, 373–390.
6. Nicholson,P. and Müller,B. (2008) Post-transcriptional control of animal histone gene expression-not so different after all. *Mol. BioSyst.*, **4**, 721–725.
7. Wang,Z.F., Whitfield,M.L., Ingledue,T.C., Dominski,Z. and Marzluff,W.F. (1996) The protein that binds the 3′ end of histone mRNA: a novel RNA-binding protein required for histone pre-mRNA processing. *Genes Dev.*, **10**, 3028–3040.
8. Martin,F., Schaller,A., Eglite,S., Schümperli,D. and Müller,B. (1997) The gene for histone RNA hairpin binding protein is located on human chromosome 4 and encodes a novel type of RNA binding protein. *EMBO J*, **15**, 769–778.
9. Schaufele,F., Gilmartin,G.M., Bannwarth,W. and Birnstiel,M.L. (1986) Compensatory mutations suggest that base-pairing with a small nuclear RNA is required to form the 3′ end of H3 messenger RNA. *Nature*, **323**, 777–781.
10. Bond,U.M., Yario,T.A. and Steitz,J.A. (1991) Multiple processing-defective mutations in a mammalian histone premessenger RNA are suppressed by compensatory changes in U7 RNA both in vivo and in vitro. *Genes Dev.*, **5**, 1709–1722.
11. Galli,G., Hofstetter,H., Stunnenberg,H.G. and Birnstiel,M.L. (1983) Biochemical complementation with RNA in the Xenopus oocyte: a small RNA is required for the generation of 3′ histone mRNA termini. *Cell*, **34**, 823–828.
12. Mowry,K.L. and Steitz,J.A. (1987) Identification of the human U7 snRNP as one of several factors involved in the 3′ end maturation of histone premessenger RNAs. *Science*, **238**, 1682–1687.
13. Soldati,D. and Schümperli,D. (1988) Structural and functional characterization of mouse U7 small nuclear RNA active in 3′ processing of histone pre-mRNA. *Mol. Cell. Biol.* **8**, 1518–1524.
14. Pillai,R.S., Grimmler,M., Meister,G., Will,C.L., Lührmann,R., Fischer,U. and Schümperli,D. (2003) Unique Sm core structure of U7 snRNPs: assembly by a specialized SMN complex and the role of a new component, Lsm11, in histone RNA processing. *Genes Dev.*, **17**, 2321–2333.
15. Pillai,R.S., Will,C.L., Lührmann,R., Schümperli,D. and Müller,B. (2001) Purified U7 snRNPs lack the Sm proteins D1 and D2 but contain Lsm10, a new 14 kDa Sm D1-like protein. *EMBO J.*, **20**, 5470–5479.
16. Dominski,Z., Erkmann,J.A., Yang,X., Sanchez,R. and Marzluff,W.F. (2002) A novel zinc finger protein is associated with U7 snRNP and interacts with the stem-loop binding protein in the histone pre-mRNP to stimulate 3′-end processing. *Genes Dev.*, **16**, 58–71.
17. Azzouz,T.N., Gruber,A. and Schümperli,D. (2005) U7 snRNP-specific Lsm11 protein: dual binding contacts with the 100 kDa zinc finger processing factor (ZFP100) and a ZFP100-independent function in histone RNA 3′ end processing. *Nucleic Acids Res.*, **33**, 2106–2117.
18. Wagner,E.J., Ospina,J.K., Hu,Y., Dundr,M., Matera,A.G. and Marzluff,W.F. (2006) Conserved zinc fingers mediate multiple functions of ZFP100, a U7snRNP associated protein. *RNA*, **12**, 1206–1218.
19. Barcaroli,D., Bongiorno-Borbone,L., Terrinoni,A., Hofmann,T.G., Rossi,M., Knight,R.A., Matera,A.G., Melino,G. and De Laurenzi,V. (2006) FLASH is required for histone transcription and S-phase progression. *Proc. Nat. Acad. Sci. U.S.A*, **103**, 14808–14812.
20. Yang,X.C., Xu,B., Sabath,I., Kunduru,L., Burch,B.D., Marzluff,W.F. and Dominski,Z. (2011) FLASH is required for the endonucleolytic cleavage of histone pre-mRNAs but is dispensable for the 5′ exonucleolytic degradation of the downstream cleavage product. *Mol. Cell. Biol.*, **31**, 1492–1502.
21. Yang,X.-C., Sabath,I., Dębski,J., Kaus-Drobek,M., Dadlez,M., Marzluff,W.F. and Dominski,Z. (2013) A Complex Containing the CPSF73 Endonuclease and Other Polyadenylation Factors Associates with U7 snRNP and Is Recruited to Histone Pre-mRNA for 3′-End Processing. *Mol. Cell. Biol.*, **33**, 28–37.
22. Ruepp,M.D., Vivarelli,S., Pillai,R., Kleinschmidt,N., Azzouz,T.N., Barabino,S.M. and Schümperli,D. (2010) The 68 kDa subunit of mammalian cleavage factor I interacts with the U7 small nuclear ribonucleoprotein and participates in 3′ end processing of animal histone mRNAs. *Nucleic Acids Res.*, **38**, 7637–7650.
23. Gick,O., Krämer,A., Vasserot,A. and Birnstiel,M.L. (1987) Heat-labile regulatory factor is required for 3′ processing of histone precursor mRNAs. *Proc. Nat. Acad. Sci. U.S.A*, **84**, 8937–8940.
24. Kolev,N.G. and Steitz,J.A. (2005) Symplekin and multiple other polyadenylation factors participate in 3′-end maturation of histone mRNAs. *Genes Dev.*, **19**, 2583–2592.
25. Romeo,V., Griesbach,E. and Schümperli,D. (2014) CstF64: Cell Cycle Regulation and Functional Role in 3′ End Processing of Replication-Dependent Histone mRNAs. *Mol. Cell. Biol.*, **34**, 4272–4284.
26. Whitfield,M.L., Zheng,L.X., Baldwin,A., Ohta,T., Hurt,M.M. and Marzluff,W.F. (2000) Stem-loop binding protein, the protein that binds the 3′ end of histone mRNA, is cell cycle regulated by both translational and posttranslational mechanisms. *Mol. Cell. Biol.*, **20**, 4188–4198.

27. Ideue,T., Adachi,S., Naganuma,T., Tanigawa,A., Natsume,T. and Hirose,T. (2012) U7 small nuclear ribonucleoprotein represses histone gene transcription in cell cycle-arrested cells. *Proc. Nat. Acad. Sci. U.S.A*, **109**, 5693–5698.
28. Tan,A.Y. and Manley,J.L. (2009) The TET Family of Proteins: Functions and Roles in Disease. *J. Mol. Cell. Biol.*, **1**, 82–92.
29. Zinszner,H., Sok,J., Immanuel,D., Yin,Y. and Ron,D. (1997) TLS (FUS) binds RNA in vivo and engages in nucleo-cytoplasmic shuttling. *J. Cell Sci.*, **110**, 1741–1750.
30. Perrotti,D., Bonatti,S., Trotta,R., Martinez,R., Skorski,T., Salomoni,P., Grassilli,E., Lozzo,R.V., Cooper,D.R. and Calabretta,B. (1998) TLS/FUS, a pro-oncogene involved in multiple chromosomal translocations, is a novel regulator of BCR/ABL-mediated leukemogenesis. *EMBO J.*, **17**, 4442–4455.
31. Baechtold,H., Kuroda,M., Sok,J., Ron,D., Lopez,B.S. and Akhmedov,A.T. (1999) Human 75-kDa DNA-pairing protein is identical to the pro-oncoprotein TLS/FUS and is able to promote D-loop formation. *J. Biol. Chem.*, **274**, 34337–34342.
32. Gardiner,M., Toth,R., Vandermoere,F., Morrice,N.A. and Rouse,J. (2008) Identification and characterization of FUS/TLS as a new target of ATM. *Biochem. J.*, **415**, 297–307.
33. Prasad,D.D., Ouchida,M., Lee,L., Rao,V.N. and Reddy,E.S. (1994) TLS/FUS fusion domain of TLS/FUS-erg chimeric protein resulting from the t(16;21) chromosomal translocation in human myeloid leukemia functions as a transcriptional activation domain. *Oncogene*, **9**, 3717–3729.
34. Lerga,A., Hallier,M., Delva,L., Orvain,C., Gallais,I., Marie,J. and Moreau-Gachelin,F. (2001) Identification of an RNA binding specificity for the potential splicing factor TLS. *J. Biol. Chem.*, **276**, 6807–6816.
35. Hoell,J.I., Larsson,E., Runge,S., Nusbaum,J.D., Duggimpudi,S., Farazi,T.A., Hafner,M., Borkhardt,A., Sander,C. and Tuschl,T. (2011) RNA targets of wild-type and mutant FET family proteins. *Nat. Struct. Mol. Biol.*, **18**, 1428–1431.
36. Colombrita,C., Onesto,E., Megiorni,F., Pizzuti,A., Baralle,F.E., Buratti,E., Silani,V. and Ratti,A. (2012) TDP-43 and FUS RNA-binding proteins bind distinct sets of cytoplasmic messenger RNAs and differently regulate their post-transcriptional fate in motoneuron-like cells. *J. Biol. Chem.*, **287**, 15635–15647.
37. Bertolotti,A., Melot,T., Acker,J., Vigneron,M., Delattre,O. and Tora,L. (1998) EWS, but Not EWS-FLI-1, Is Associated with Both TFIID and RNA Polymerase II: Interactions between Two Members of the TET Family, EWS and hTAFII68, and Subunits of TFIID and RNA Polymerase II Complexes. *Mol. Cell. Biol.*, **18**, 1489–1497.
38. Zinszner,H., Albalat,R. and Ron,D. (1994) A novel effector domain from the RNA-binding protein TLS or EWS is required for oncogenic transformation by CHOP. *Genes Dev.*, **8**, 2513–2526.
39. Hallier,M., Lerga,A., Barnache,S., Tavitian,A. and Moreau-Gachelin,F. (1998) The Transcription Factor Spi-1/PU.1 Interacts with the Potential Splicing Factor TLS. *J. Biol. Chem.*, **273**, 4838–4842.
40. Powers,C.A., Mathur,M., Raaka,B.M., Ron,D. and Samuels,H.H. (1998) TLS (Translocated-in-Liposarcoma) Is a High-Affinity Interactor for Steroid, Thyroid Hormone, and Retinoid Receptors. *Mol. Endocrinol.*, **12**, 4–18.
41. Tan,A.Y. and Manley,J.L. (2010) TLS Inhibits RNA Polymerase III Transcription. *Mol. Cell. Biol.*, **30**, 186–196.
42. Hackl,W., Fischer,U. and Lührmann,R. (1994) A 69-kD protein that associates reversibly with the Sm core domain of several spliceosomal snRNP species. *J. Cell Biol.*, **124**, 261–272.
43. Yang,L., Embree,L.J., Tsai,S. and Hickstein,D.D. (1998) Oncoprotein TLS Interacts with Serine-Arginine Proteins Involved in RNA Splicing. *J. Biol. Chem.*, **273**, 27761–27764.
44. Rappsilber,J., Ryder,U., Lamond,A.I. and Mann,M. (2002) Large-scale proteomic analysis of the human spliceosome. *Genome Res.*, **12**, 1231–1245.
45. Zhou,Z., Licklider,L.J., Gygi,S.P. and Reed,R. (2002) Comprehensive proteomic analysis of the human spliceosome. *Nature*, **419**, 182–185.
46. Meissner,M., Lopato,S., Gotzmann,J., Sauermann,G. and Barta,A. (2003) Proto-oncoprotein tls/fus is associated to the nuclear matrix and complexed with splicing factors ptb, srm160, and sr proteins. *Exp. Cell Res.*, **283**, 184–195.
47. Ishigaki,S., Masuda,A., Fujioka,Y., Iguchi,Y., Katsuno,M., Shibata,A., Urano,F., Sobue,G. and Ohno,K. (2012) Position-dependent FUS-RNA interactions regulate alternative splicing events and transcriptions. *Sci. Rep.*, **2**, 529.
48. Lagier-Tourenne,C., Polymenidou,M., Hutt,K.R., Vu,A.Q., Baughn,M., Huelga,S.C., Clutario,K.M., Ling,S.-C., Liang,T.Y., Mazur,C. *et al.* (2012) Divergent roles of ALS-linked proteins FUS/TLS and TDP-43 intersect in processing long pre-mRNAs. *Nat. Neurosci.*, **15**, 1488–1497.
49. Sun,S., Ling,S.-C., Qiu,J., Albuquerque,C.P., Zhou,Y., Tokunaga,S., Li,H., Qiu,H., Bui,A., Yeo,G.W. *et al.* (2015) ALS-causative mutations in FUS/TLS confer gain and loss of function by altered association with SMN and U1-snRNP. *Nat. Commun.*, **6**, 6161.
50. Gregory,R.I., Yan,K.-P., Amuthan,G., Chendrimada,T., Doratotaj,B., Cooch,N. and Shiekhattar,R. (2004) The Microprocessor complex mediates the genesis of microRNAs. *Nature*, **432**, 235–240.
51. Kwiatkowski,T.J., Bosco,D.A., LeClerc,A.L., Tamrazian,E., Vanderburg,C.R., Russ,C., Davis,A., Gilchrist,J., Kasarskis,E.J., Munsat,T. *et al.* (2009) Mutations in the FUS/TLS Gene on Chromosome 16 Cause Familial Amyotrophic Lateral Sclerosis. *Science*, **323**, 1205–1208.
52. Vance,C., Rogelj,B., Hortobágyi,T., De Vos,K.J., Nishimura,A.L., Sreedharan,J., Hu,X., Smith,B., Ruddy,D., Wright,P. *et al.* (2009) Mutations in FUS, an RNA Processing Protein, Cause Familial Amyotrophic Lateral Sclerosis Type 6. *Science*, **323**, 1208–1211.
53. Lagier-Tourenne,C., Polymenidou,M. and Cleveland,D.W. (2010) TDP-43 and FUS/TLS: emerging roles in RNA processing and neurodegeneration. *Hum. Mol. Genet.*, **19**, R46–R64.
54. Neumann,M. (2013) Frontotemporal lobar degeneration and amyotrophic lateral sclerosis: molecular similarities and differences. *Rev. Neurol. (Paris)*, **169**, 793–798.
55. Neumann,M., Bentmann,E., Dormann,D., Jawaid,A., DeJesus-Hernandez,M., Ansorge,O., Roeber,S., Kretzschmar,H.A., Munoz,D.G., Kusaka,H. *et al.* (2011) FET proteins TAF15 and EWS are selective markers that distinguish FTLD with FUS pathology from amyotrophic lateral sclerosis with FUS mutations. *Brain.*, **134**, 2595–2609.
56. Wiznerowicz,M. and Trono,D. (2003) Conditional suppression of cellular genes: lentivirus vector-mediated drug-inducible RNA interference. *J. Virol.*, **77**, 8957–8961.
57. Ariumi,Y., Turelli,P., Masutani,M. and Trono,D. (2005) DNA Damage Sensors ATM, ATR, DNA-PKcs, and PARP-1 Are Dispensable for Human Immunodeficiency Virus Type 1 Integration. *J. Virol.*, **79**, 2973–2978.
58. Metze,S., Herzog,V.A., Ruepp,M.-D. and Mühlemann,O. (2013) Comparison of EJC-enhanced and EJC-independent NMD in human cells reveals two partially redundant degradation pathways. *RNA*, **19**, 1432–1448.
59. Brummelkamp,T.R., Bernards,R. and Agami,R. (2002) A system for stable expression of short interfering RNAs in mammalian cells. *Science*, **296**, 550–553.
60. Paillusson,A., Hirschi,N., Vallan,C., Azzalin,C.M. and Mühlemann,O. (2005) A GFP-based reporter system to monitor nonsense-mediated mRNA decay. *Nucleic Acids Res.*, **33**, e54.
61. Lerner,E.A., Lerner,M.R., Janeway,C.A. and Steitz,J.A. (1981) Monoclonal antibodies to nucleic acid-containing cellular constituents: probes for molecular biology and autoimmune disease. *Proc. Natl. Acad. Sci. U.S.A.*, **78**, 2737–2741.
62. Zhou,Z. and Reed,R. (2003) Purification of functional RNA-protein complexes using MS2-MBP. In: *Current Protocols in Molecular Biology*. John Wiley & Sons, Inc, Hoboken, NJ.
63. Blum,H., Beier,H. and Gross,H.J. (1987) Improved silver staining of plant proteins, RNA and DNA in polyacrylamide gels. *Electrophoresis*, **8**, 93–99.
64. Al Kaabi,A., Traupe,T., Stutz,M., Buchs,N. and Heller,M. (2012) Cause or effect of arteriogenesis: compositional alterations of microparticles from CAD patients undergoing external counterpulsation therapy. *PloS one*, **7**, e46822.
65. Engel,H., Mika,M., Denapaite,D., Hakenbeck,R., Mühlemann,K., Heller,M., Hathaway,L.J. and Hilty,M. (2014) A Low-Affinity Penicillin-Binding Protein 2x Variant Is Required for Heteroresistance in Streptococcus pneumoniae. *Antimicrob. Agents Chemother.*, **58**, 3934–3941.
66. Bühler,M., Steiner,S., Mohn,F., Paillusson,A. and Mühlemann,O. (2006) EJC-independent degradation of nonsense

immunoglobulin-mu mRNA depends on 3′ UTR length. *Nat. Struct. Mol. Biol.*, **13**, 462–464.
67. Thermann,R., Neu-Yilik,G., Deters,A., Frede,U., Wehr,K., Hagemeier,C., Hentze,M.W. and Kulozik,A.E. (1998) Binary specification of nonsense codons by splicing and cytoplasmic translation. *EMBO J.*, **17**, 3484–3494.
68. Yamazaki,T., Chen,S., Yu,Y., Yan,B., Haertlein,TylerC., Carrasco,Monica A., Tapia,JuanC., Zhai,B., Das,R., Lalancette-Hebert,M. *et al.* (2012) FUS-SMN Protein Interactions Link the Motor Neuron Diseases ALS and SMA. *Cell Rep.*, **2**, 799–806.
69. Gerbino,V., Carrì,M.T., Cozzolino,M. and Achsel,T. (2013) Mislocalised FUS mutants stall spliceosomal snRNPs in the cytoplasm. *Neurobiol. Dis.*, **55**, 120–128.
70. Ruepp,M.D., Schweingruber,C., Kleinschmidt,N. and Schümperli,D. (2011) Interactions of CstF-64, CstF-77, and symplekin: Implications on localisation and function. *Mol. Biol. Cell*, **22**, 91–104.
71. Kari,V., Karpiuk,O., Tieg,B., Kriegs,M., Dikomey,E., Krebber,H., Begus-Nahrmann,Y. and Johnsen,S.A. (2013) A Subset of Histone H2B Genes Produces Polyadenylated mRNAs under a Variety of Cellular Conditions. *PloS one*, **8**, e63745.
72. Zhao,J., Kennedy,B.K., Lawrence,B.D., Barbie,D.A., Matera,A.G., Fletcher,J.A. and Harlow,E. (2000) NPAT links cyclin E-Cdk2 to the regulation of replication-dependent histone gene transcription. *Genes Dev.*, **14**, 2283–2297.
73. Pirngruber,J. and Johnsen,S.A. (2010) Induced G1 cell-cycle arrest controls replication-dependent histone mRNA 3[prime] end processing through p21, NPAT and CDK9. *Oncogene*, **29**, 2853–2863.
74. Marzluff,W.F., Gongidi,P., Woods,K.R., Jin,J. and Maltais,L.J. (2002) The Human and Mouse Replication-Dependent Histone Genes. *Genomics*, **80**, 487–498.
75. Zheng,L., Roeder,R.G. and Luo,Y. (2003) S Phase Activation of the Histone H2B Promoter by OCA-S, a Coactivator Complex that Contains GAPDH as a Key Component. *Cell*, **114**, 255–266.
76. Miele,A., Braastad,C.D., Holmes,W.F., Mitra,P., Medina,R., Xie,R., Zaidi,S.K., Ye,X., Wei,Y., Harper,J.W. *et al.* (2005) HiNF-P Directly Links the Cyclin E/CDK2/p220NPAT Pathway to Histone H4 Gene Regulation at the G1/S Phase Cell Cycle Transition. *Mol. Cell. Biol.*, **25**, 6140–6153.
77. Kim,S.H., Shanware,N.P., Bowler,M.J. and Tibbetts,R.S. (2010) Amyotrophic Lateral Sclerosis-associated Proteins TDP-43 and FUS/TLS Function in a Common Biochemical Complex to Co-regulate HDAC6 mRNA. *J. Biol. Chem.*, **285**, 34097–34105.
78. Bentley,D.L. (2005) Rules of engagement: co-transcriptional recruitment of pre-mRNA processing factors. *Curr. Opin. Cell Biol.*, **17**, 251–256.
79. Adamson,T.E. and Price,D.H. (2003) Cotranscriptional processing of Drosophila histone mRNAs. *Mol.Cell Biol.*, **23**, 4046–4055.
80. Hsin,J.P., Sheth,A. and Manley,J.L. (2011) RNAP II CTD Phosphorylated on Threonine-4 Is Required for Histone mRNA 3′ End Processing. *Science*, **334**, 683–686.
81. Hintermair,C., Heidemann,M., Koch,F., Descostes,N., Gut,M., Gut,I., Fenouil,R., Ferrier,P., Flatley,A., Kremmer,E. *et al.* (2012) Threonine-4 of mammalian RNA polymerase II CTD is targeted by Polo-like kinase 3 and required for transcriptional elongation. *EMBO J.*, **31**, 2784–2797.
82. Heidemann,M., Hintermair,C., Voss,K. and Eick,D. (2013) Dynamic phosphorylation patterns of RNA polymerase II CTD during transcription. *Biochim. Biophys. Acta.*, **1829**, 55–62.
83. He,H., Yu,F.-X., Sun,C. and Luo,Y. (2011) CBP/p300 and SIRT1 are involved in transcriptional regulation of S-phase specific histone genes. *PloS one*, **6**, e22088.
84. Zhao,J., Dynlacht,B., Imai,T., Hori,T.-A. and Harlow,E. (1998) Expression of NPAT, a novel substrate of cyclin E–CDK2, promotes S-phase entry. *Genes Dev.*, **12**, 456–461.
85. Wei,Y., Jin,J. and Harper,J.W. (2003) The Cyclin E/Cdk2 Substrate and Cajal Body Component p220NPAT Activates Histone Transcription through a Novel LisH-Like Domain. *Mol. Cell. Biol.*, **23**, 3669–3680.
86. Schwartz,J.C., Ebmeier,C.C., Podell,E.R., Heimiller,J., Taatjes,D.J. and Cech,T.R. (2012) FUS binds the CTD of RNA polymerase II and regulates its phosphorylation at Ser2. *Genes Dev.*, **26**, 2690–2695.